JOURNAL OF MORPHOLOGY 259:281–307 (2004)

Relationships of Loading History and Structural and Material Characteristics of Bone: Development of the Mule Deer Calcaneus

John G. Skedros,* Kenneth J. Hunt, and Roy D. Bloebaum

Bone and Joint Research Laboratories (151F), Department of Veterans Affairs Medical Center, Salt Lake City, Utah 84148

ABSTRACT If a bone's morphologic organization exhibits the accumulated effects of its strain history, then the relative contributions of a given strain stimulus to a bone's development may be inferred from a bone's hierarchical organization. The artiodactyl calcaneus is a short cantilever, loaded habitually in bending, with prevalent compression in the cranial (Cr) cortex, tension in the caudal (Cd) cortex, and shear in the medial and lateral cortices (i.e., neutral axis). Artiodactyl calcanei demonstrate unusually heterogeneous structural and material organization between these cortices. This study examines potential relationships between developmental morphologic variations and the functional strain distribution of the deer calcaneus. One calcaneus was obtained from each of 36 (fetus to adult) wild deer. Predominant collagen fiber orientation (CFO), microstructural characteristics, mineral content (% ash), and geometric parameters were determined from transversely cut segments. Radiographs were examined for arched trabeculae, which may reflect tension/compression stress trajectories. Results showed that cross-sectional shape changes with age from quasi-circular to quasi-elliptical, with the long axis in the cranial–caudal direction of habitual bending. Cranial ("compression") cortical thickness increased at a greater rate than the Cd ("tension") cortex. Fetal bones exhibited arched trabeculae. Percent ash was *not* uniform (Cr > Cd), and this disparity increased with age (absolute differences: 2.5% fetuses, 4.3% adults). Subadult bones showed progressively more secondary osteons and osteocyte lacunae in the Cr cortex, but the Cd cortex tended to have more active remodeling in the subadult and adult bones. Nonuniform Cr:Cd CFO patterns first consistently appear in the subadults, and are correlated with secondary bone formation and habitual strain mode. Medial and lateral cortices in these groups exhibited elongated secondary osteons. These variations may represent "strain-mode-specific" (i.e., tension, compression, shear) adaptations. The heterogeneous organization may also be influenced by variations in longitudinal strain magnitude (highest in the Cr cortex) and principal strain direction—oblique in medial-lateral cortices (where shear strains also predominate). Other factors such as local reductions in longitudinal strain may influence the increased remodeling activity of the Cd cortex. Some structural variations, such as arched trabeculae, that are established early in ontogeny may be strongly influenced by genetic- or epigenetic-derived processes. Material variations, such as secondary osteon population densities and CFO, which appear later, may be products of extragenetic factors, including microdamage. J. Morphol. 259:281–307, 2004.

KEY WORDS: bone adaptation; mineral content; mule deer calcaneus; osteons; collagen fiber orientation; osteocyte lacuna; cortical thickness

A growing body of experimental data suggests that bone tissue can exhibit the accumulated effects of its strain history* (Lanyon and Baggott, 1976; Carter et al., 1980; Carter, 1984, 1987; Burr, 1992; Riggs et al., 1993a,b; Levenston, 1994; Levenston et al., 1994; van der Meulen et al., 1996; Reilly et al., 1997; Skedros and Kuo, 1999; Skedros et al., 1996a, 1999, 2001a,b). In this context, it has been suggested that the relative contributions of a given strain stimulus to appendicular skeletal development may be

Contract grant sponsors: Office of Research and Development (R&D) Medical Research Service, Department of Veterans Affairs (VA) Salt Lake City Health Care System, the Department of Orthopaedics, University of Utah School of Medicine, the Orthopaedic Research and Education Foundation; Contract grant number: 01-024; Contract grant sponsor: the Utah Bone and Joint Center.

*Correspondence to: John G. Skedros, M.D., Bone and Joint Research Laboratories (151F), Department of Veterans Affairs Medical Center, 500 Foothill Blvd., Salt Lake City, UT, 84148.
E-mail: jskedros@utahboneandjoint.com

*Mechanical strain is the change in length of a loaded structure as a percentage of its initial (unloaded) length. This dimensionless ratio is a measure of material or tissue deformation. In vivo strain data on a variety of animals suggest that physiologically normal strains are generally between 200 and 3,000 microstrain (i.e., between 0.02% and 0.30% change in length) in compression (Rubin and Lanyon, 1985; Biewener et al., 1983a,b, 1986). The upper limit may be only 1,500 microstrain in tension (Fritton and Rubin, 2001). For an isotropic material loaded axially, stress and strain are related by Hooke's law, which says that they are proportional to one another. Available data suggest that strain is the mechanical parameter most directly involved in mediating bone adaptations (Rubin and Lanyon, 1984; Lanyon, 1987).

DOI: 10.1002/jmor.10167

TABLE 1. Predicted developmental structural and material changes of the mule deer calcaneus fetal fawn to adult

	Predicted changes	
	Young fawns	Adults
Structural characteristics		
Cross-sectional shape	Circular	Elliptical (with long axis in cranial-caudal direction)
Cortical thickness	Regionally uniform[a]	Thickest cortex: cranial; Equal medial and lateral cortices
Cortical area		Increased % of total cross-sectional area (i.e., increased robusticity)
Trabecular bone	Lack of arched patterns in lateral view (fetal bones)	Presence of arched patterns in lateral view
Material characteristics		
Mineral content (%ash)	Generally lower[b]	Generally higher
	Regionally uniform	Highest in cranial cortex
		Lowest in caudal cortex
		Intermediate in medial/lateral cortices
Porosity (Po/Ar)	Generally high	Lowest in cranial cortex
	Regionally uniform	Highest in caudal cortex
2nd osteon pop. density[c] (N.On/Ar)	Few or none	Generally high with non-uniform distribution
		Highest in cranial cortex
New remodeling events[d] (NREs)	Generally high	Generally low
	Regionally uniform	Highest in caudal cortex
Osteocyte lacuna pop. density[c] (N.Lac/Ar)	Regionally uniform	Highest in cranial cortex
Predominant CFO[c]	Regionally uniform	Oblique-to-transverse in cranial cortex
	No apparent strain-mode relationship[c]	Longitudinal in caudal cortex

[a]"Regionally uniform" means roughly equivalent in the cranial, caudal, medial, and lateral cortices.
[b]"Generally" refers to the entire cross section (i.e., all regions analyzed).
[c]pop., population; CFO, collagen fiber orientation; strain mode, tension, compression, shear.
[d]New remodeling events (NREs), newly forming secondary osteons and resorption spaces

inferred from one or more specific characteristics of a bone's hierarchical organization (e.g., Table 1) (Currey, 1984a; Martin and Burr, 1989; Bromage, 1992; McMahon et al., 1995; Skedros et al., 1996a, 1997; Skedros, 2001). It also has been suggested that within the detailed structure of a bone, one can detect evidence of its load history (Skerry et al., 1990; Brand, 1992; Riggs et al., 1993a,b; Mason et al., 1995; Skedros and Kuo, 1999; Takano et al., 1999; Skedros et al., 1994a,b, 1996a, 1998, 1999, 2002a). Thus, a bone's hierarchical structural and material organization may embody a record or "history" of important aspects of past and/or current loading conditions (Skerry et al., 1990; Brand, 1992; Riggs et al., 1993a,b; Alberts, 1994; Levenston et al., 1994; Mason et al., 1995; Takano et al., 1999; Skedros, 2001; Skedros et al., 2001a). Consistent and relatively long strain histories are expected in many appendicular bones since in vivo strain gauge measurements from various mammalian and avian species typically demonstrate directionally constrained, habitual bending—producing a spatially consistent tension/compression/shear strain distribution during peak loading of controlled physiologic activities regardless of the animal's ontogenetic stage of development (Lanyon and Baggott, 1976; Lanyon et al., 1979; Biewener et al., 1986; Indrekvam et al., 1991; Biewener and Bertram, 1993). Empirical strain data also show that habitual bending is not only highly conserved in functional loading of diaphyses of many appendicular long bones, but bending also produces the majority (>70%) of longitudinal strains occurring during controlled in vivo activity (Lanyon and Baggott, 1976; Lanyon et al., 1979; Biewener et al., 1986; Indrekvam et al., 1991; Biewener and Bertram, 1993).

It has been suggested that regional variations in cortical bone morphology would be most evident in limb bone diaphyses habitually loaded in bending (Skedros et al., 1996a, 2001a). This may be because the mechanical properties and fracture and microdamage mechanics of cortical bone markedly differ in tension, compression, and shear (Reilly and Burstein, 1974, 1975; Burstein et al., 1972, 1976; Carter and Hayes, 1977; O'Connor et al., 1982; Norman et al., 1995, 1996; Pattin et al., 1996; Jepsen and Davy, 1997; Yeni et al., 1997; Boyce et al., 1998; Burr et al., 1998; Huja et al., 1999; Reilly and Currey, 1999, 2000; Brown et al., 2000; Jepsen et al., 2001; Turner et al., 2001). Consequently, a compelling case can be made for examining a bone with tension predominating in one cortex, compression predominating in the opposite cortex, and shear predominating along the neutral axis for inferring causal relationships between local strain histories and limb bone organization.

The artiodactyl calcaneus has been described as a simply loaded "tension/compression" bone (Su et al., 1999; Skedros et al., 1994a,b, 1997, 2001a, 2002a) (Fig. 1). In vivo and in vitro data demonstrate that, during physiologic weight-bearing activities, the calcaneal diaphysis behaves like a short-cantilevered

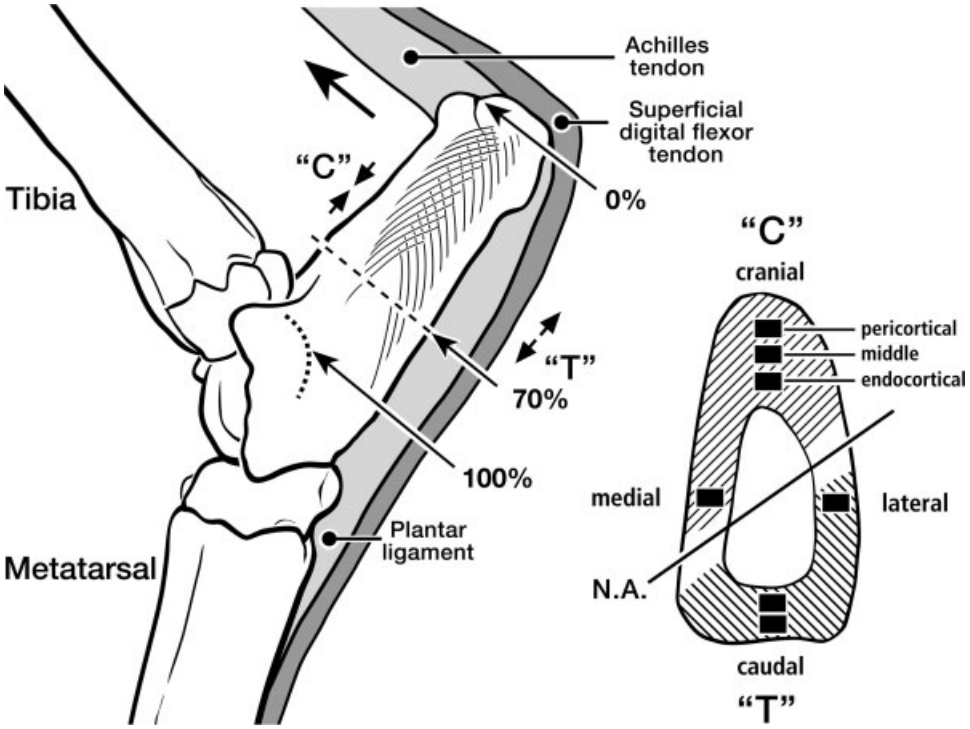

Fig. 1. Lateral-to-medial view of the ankle region of a skeletally mature mule deer showing the calcaneus, shaft length, and other associated bones, ligaments, and tendons. The trabecular patterns are stylized and are based on a medial-to-lateral roentgenogram. The dotted line at the tip of the 100% arrow indicates the projected location of the contour formed by the talus-calcaneus articular surfaces. The large cranial-directed arrow indicates the direction of force imparted by the Achilles tendon during mid-stance, loading the cranial cortex in compression ("C") and caudal cortex in tension ("T") (Su et al., 1999). The cross-section is from a 70% section and shows the location from which the microscopic images were taken and the approximate location of the neutral axis (NA).

beam with longitudinal compression and tension strains predominating on opposing cranial and caudal cortices, respectively (Lanyon, 1974; Su et al., 1999). Recent studies have shown that artiodactyl calcanei have unusually heterogeneous structural and material organization between cortical regions of the same transverse cross-section (Skedros et al., 1993a, 1994a,b, 1997, 2001a). For example, subadult and mature mule deer calcanei exhibit biomechanically significant regional differences in cortical thickness, mineral content (% ash), microstructure (e.g., porosity, new osteon remodeling events, and secondary osteon cross-sectional shape and population densities), and ultrastructure (e.g., predominant collagen fiber orientation and collagen molecular cross-links) (see Appendix for definitions) (Gunasekaran et al., 1991; Skedros, 1994, 2000, 2001; Skedros et al., 1994a,b, 2001a,d, 2003a). In fact, to our knowledge the differences in % ash that occur between cranial–caudal cortical regions of mature deer calcanei are the *largest* that have been described *within the same cross section* of a mature limb bone of any vertebrate taxon. It has been speculated that these unusually conspicuous morphologic heterogeneities represent the outcome of adaptive bone modeling and remodeling responses to a long history of the functional cranial–caudal compression–tension strain distribution. Consequently, the artiodactyl calcaneus is being promoted as an experimental model for investigating the mechanisms that govern the modeling and remodeling processes that produce and maintain functionally adapted bone (Skedros et al., 2001a). Although structural and material organizations of mature and subadult mule deer calcanei have been described, little is known about the material modifications that occur during their earlier development.

The objectives of the present study are to: 1) further examine the ontogenetic structural and material development of the mule deer calcaneus, and 2) establish relationships between developmental morphologic modifications and the functional strain distribution in the mule deer calcaneus model. Hypothesized ontogenetic changes are shown in Table 1.

In addition to investigating these hypotheses, we also considered the following questions:

1) Do regional and ontogenetic differences reflect a habitual nonuniform strain distribution that begins in utero?
2) What functions do the regional material heterogeneities serve; or, what would be the consequences if similar material organization was maintained throughout a cross section and only bone microstructure was modified?
3) Is the progressive reorganization of material characteristics a response to regional differences in various components of a bone's habitual strain history (e.g., strain magnitudes, modes, and directions)?
4) What alternative explanations, other than strain transduction, might be offered to explain the mechanisms that mediate these variations?

TABLE 2. Specimen age groups

Length	Age group	n
<2.9 cm	Younger fawns	9
3.0–4.4 cm	Older fawns	6
4.5–6.02 cm	Subadults	11
>6.03 cm*	Adults	10

*Specimens were considered "adults" if length was greater than 6.03 cm *and* there was gross evidence of distal growth plate closure.

MATERIALS AND METHODS
Mule Deer Calcaneus Model: Strain Data

Among common artiodactyl calcanei, the mule deer calcaneus (Fig. 1) is one of the most beam-like (Schmid, 1972). Su and colleagues (Su, 1998; Su et al., 1999) performed rigorous in vitro strain analyses on mule deer calcanei using up to seven rosette strain gauges on one bone. During simulated mid-stance phase of various gaits, the cranial calcaneus exhibits peak compressive strains on the order of 350 to 1,100 με (491N to 1962N end load, respectively) and the caudal calcaneus exhibits estimated peak tensile strains on the order of 380 to 940 με (491N to 1962N end load, respectively) (491N and 1962N correspond to ~0.3 and 1.0 times body weight, respectively). At these loads, strains on the medial and lateral cortices were also notable (medial: 390–1,330 με in compression; lateral: 350–1,170 με in tension) even though these regions are considered to be on a neutral axis where longitudinal strains are minimal. These results reflect the fact that the axis of peak strains along these medial and lateral locations are significantly *oblique* to the bone's longitudinal axis (Su et al., 1999) (Fig. 1). (Consequently, shear strains in these regions, when compared to the cranial and caudal cortices, are more closely aligned with the longitudinal axis of the bone.) Su et al. (1999) also showed that caudal cortex strains were predominately tensile, even with an intact plantar ligament. The customary tension–compression strain milieu of the mule deer calcaneus also resembles in vivo strain milieus of ovine (*Ovis* sp.) and potoroo (*Potorous tridactylus,* a small marsupial) calcanei (Lanyon, 1974; Biewener et al., 1996; Su et al., 1999), which are similarly loaded, short, cantilevered, beam-like bones.

Specimens

One calcaneus was obtained from each of 36 wild Rocky Mountain mule deer (*Odocoileus hemionus hemionus*). The animals represented an age range from fetus to adult (Table 2). In nearly all cases animal mass was not available. Most of the subadult animals were found dead at a roadside in mountainous terrain of northern Utah. The two fetuses were near-term twins (2.2 ± 0.1 kg) that were obtained from a pregnant doe that had been hit by an automobile. Although gender was not determined in the younger animals, the older subadult and adult animals were all males and were collected from a game-processing facility (Davis County, Utah, USA) during late October of a fall hunting season. Because growth rates and body mass of male and female mule deer diverge between 12 and 18 months postpartum (Anderson, 1981), no bones belonging to females older than a young subadult were included in this study. Using a knife, soft tissues were manually removed from all bones.

Based on the presence or absence of a co-ossified distal growth plate near the insertion of the Achilles tendon (Purdue, 1983), the paired calcanei were separated into skeletally immature (n = 26) and mature (n = 10) bones. As described below, the subadult group was further subdivided into younger fawns (including fetal, n = 9), older fawns (n = 6), and subadults (n = 11).

At the time of specimen collection from subadult and adult animals, the periosteal ("velvet") covering of the antlers had been shed and antler growth was complete, and the animals had not yet participated in aggressive physical interactions characteristic of the rut (Anderson, 1981; Goss, 1983). These facts diminish the possibility that current remodeling activities of the adult animals are the result of metabolic demands of antler growth and/or repair of bone microdamage caused during the rut.

Radiography

Each calcaneus was radiographed in the medial-to-lateral projection. The radiographs were examined for the presence or absence of the arched patterns of trabeculae that have been described in mature animals and have been described as adaptations for tension and compression stress trajectories (Lanyon, 1974; Skedros and Brady, 2001; Skedros et al., 2001a, 2002b).

Shaft Length, Age Segregation, and Sectioning

After radiography, diaphyseal "length" of each bone was measured using a digital vernier caliper (Mitutoyo, Japan) (Fig. 1). Based on these length measurements, the following age groups were arbitrarily created: 1) young fawns (<2.9 cm); 2) older fawns (3.0–4.4 cm); 3) subadults (4.5–6.02 cm *and* the presence of a cartilaginous growth plate at the distal end); and 4) adults (>6.03 cm *and* an ossified distal growth plate) (Table 2). It should be noted that three subadult bones exceeded 6.02 cm (i.e., 6.23, 6.25, 6.40 cm).

Although we could not locate information regarding animal age at epiphyseal closure in limb bones of Rocky Mountain mule deer, comparative data are available in the black-tailed deer subspecies (*Odocoileus hemionus columbianus*). Lewall and Cowan (1963) and Purdue (1983) reported that the distal epiphyseal growth plates of calcanei of white- and black-tailed deer are half-fused by ~20–26 months postpartum. Based on these data, we estimate that epiphyseal closure in the calcaneus is consistent with an estimated age range of 1.5–3 years for the subadult Rocky Mountain mule deer.

Transverse cuts were made along the calcaneal diaphysis producing 3–6 mm thick segments between the 50% and 60% locations (the "50% segment"), 60% and 70% locations (the "60% segment"), and 70% and 80% locations (the "70% segment"). The 70% segment is closest to the joint surface (Skedros et al., 1994a; Fig. 1). The 60% segments were measured for cortical thickness, medial–lateral "width" and cranial–caudal "height." As described below, cortical thickness, cross-sectional geometric, and % ash measurements were made on the 60% segments and microstructural analyses were conducted on the 50% and 70% segments.

Cortices and Cortical Regions—Terminology and Abbreviations

Abbreviations appear in Table 3. Microstructural and ultrastructural measurements were made at the cranial, caudal, medial, and lateral locations. The intracortical "envelopes" (pericortical, middle, endocortical) will be referred to as "regions" (periosteal, middle, endosteal) (Fig. 1). The medial and lateral cortices are also described as "neutral axis" or "shear" regions (Skedros et al., 2001a).

Cortical Thickness

Thickness of cranial, caudal, medial, and lateral cortices of the 60% segments were measured to within ±0.01 mm. Subperiosteal cranial–caudal "heights" and medial–lateral "widths" of each segment were also measured; medial–lateral width was measured midway between the cranial and caudal endosteal margins of the medullary canal.

TABLE 3. Abbreviations

CFO	= Predominant collagen fiber orientation expressed asWMGL (see below)Cort.Th = Cortical thickness (mm)
Imax	= Major axis of second moment of inertia (mm^4)
Imin	= Minor axis of second moment of area (mm^4)
CA	= Cortical Area (mm^2)
TA	= Total cross-sectional area (mm^2)
J	= Polar moment of inertia (mm^4)
Z	= Section modulus (mm^3)
%Ash	= Mineral content
N.On/Ar	= Secondary osteon population density (no./mm^2)
Lac.Ar	= Mean cross-sectional area of osteocyte lacunae (μm^2)
N. Lac/Ar	= Osteocyte lacuna population density (no./mm^2)
On.B/Ar	= Fractional area of secondary osteonal bone × 100 (%)
Po/Ar	= Fractional area of non-lacunar porous spaces × 100 (%)
WMGL	= Weighted mean graylevel (larger numbers indicate more oblique-to-transverse collagen, smaller numbers indicate more longitudinal collagen) (See CFO above)
NREs	= New remodeling events (resorption spaces plus newly forming osteons) (no./mm^2)

Mineral Content (% Ash)

Using a diamond-blade saw with continuous water irrigation, 3–4-mm wide fragments spanning the entire cortex of bone were obtained from cranial, caudal, medial, and lateral aspects of each 60% cross-sectional segment. The immediate subperiosteal and subendosteal bone was removed from each fragment by manual surface abrasion in order to exclude fibrous tissue associated with the periosteum (cranial cortex), plantar ligament insertion (caudal cortex), or endosteum (medullary canal), which would artifactually lower mineral content.

Dry and ash weights were obtained for all four cortical fragments of each specimen using previously described methods (Skedros et al., 1993b). Mineral content (% ash) was calculated by dividing the weight of the ashed bone (W_{AB}) by the weight of the dried, defatted bone (W_{DB}) prior to ashing and multiplying this quotient by 100 [$(W_{AB}/W_{DB}) \cdot 100$].

Microstructure

Microstructural analyses were conducted on the distal cut surfaces of the 50% and 70% segments (Skedros et al., 1994a). These segments were embedded in polymethyl methacrylate (Emmanual et al., 1987) and prepared for imaging in the backscattered electron (BSE) mode of a scanning electron microscope (Skedros et al., 1993a,b). In specimens with sufficient cortical area, one 50× image (1.6 × 2.3 mm) and two 100× (0.8 × 1.1 mm) images were obtained in each periosteal, middle, and endosteal region of each cranial and caudal cortex. Similarly, one 50× and two 100× images were also obtained in each of the medial and lateral cortices (Fig. 1). In the smaller bones, only 100× image areas were required.

Using conventional point counting techniques and methods described by Skedros et al. (1994b), fractional area of secondary osteonal bone (osteonal bone per area, On.B/Ar) and population densities of new remodeling events (NREs = resorption spaces and newly forming secondary osteons (no./mm^2)) were determined in each 50× image. The On.B/Ar was defined as the total area of secondary bone (S) divided by the total area of secondary bone plus interstitial bone (I), [S/(S+I)]. Secondary osteon population density (number of secondary osteons per area, N.On/Ar; no./mm^2), and porosity (Po/Ar) were determined in each 100× image (Skedros et al., 1994b).

Newly forming secondary osteons were identified using two criteria: 1) the presence of relatively recently mineralized bone (seen as relatively darker graylevels in the BSE images), and 2) incomplete radial closure (i.e., incomplete centripetal deposition) of the recently mineralized bone. To determine if the second criterion was satisfied, two mutually orthogonal lines (cranial–caudal and medial–lateral directions) were drawn on each apparent newly forming osteon. Incomplete radial closure was defined as mineralized bone extending less than one-half of the osteon radius along two or more of the four possible radial locations (i.e., cranial, caudal, medial, or lateral). Complete and fragmented secondary osteons and NREs were identified by one investigator and confirmed independently by a second investigator.

Backscattered electron images were also examined for the presence of hypermineralized tissue consistent with calcified cartilage, which may be present during earlier phases of endochondral osteogenesis.

Circularly Polarized Light Analysis

A 1-mm-thick section was obtained from the PMMA-embedded 50% and 70% segments of a subset (n = 21) of bones representing a range from fetus to adult. These sections were ultramilled to 100 ± 5 μ and analyzed for predominant collagen fiber orientation (CFO) using circularly polarized light according to published methods (Boyde and Riggs, 1990; Skedros et al., 1996a). Regional differences in CFO were quantified in terms of corresponding differences in the transmitted light intensity, where darker graylevels (lower numerical values) represent relatively more longitudinal CFO and brighter graylevels (higher numerical values) represent relatively more oblique-to-transverse CFO. The methods used to quantify regional CFO differences in cortical bone as differences in graylevels (Skedros et al., 1996) have produced relative differences that are similar to the "longitudinal structure index" described by Martin and co-workers (Martin and Burr, 1989; Martin et al., 1996) and recently used by Takano et al. (1999) and Kalmey and Lovejoy (2002).

Geometric Analyses

Tracings of endosteal and periosteal perimeters of the 60% cross-sectional segments were digitized using a high-resolution scanner (Hewlett Packard, ScanJet 6100C) interfaced with a microcomputer. An algorithm created for the public domain NIH image (v. 1.61) software (developed at the U.S. National Institutes of Health and available on the Internet at http://rsb.info.nih.gov/nih-image/ or on floppy disk from the National Information Service, Springfield, VA [part number PB95-500195GEI]; the PC version is entitled "Scion image" and can be downloaded from http://www.scioncorp.com), and adapted from the computer program SLICE (Nagurka and Hayes, 1980), was then used to determine the following from each tracing: 1) total subperiosteal area (TA in mm^2); 2) cortical area (CA, in mm^2); and 3) major axis (Imax, in mm^4) and orthogonal minor axis (Imin, in mm^4) of the second moment of area (inertia, I). Polar moment of inertia (J) was also calculated for each section (J = Imax + Imin, in mm^4).

According to engineering principles applied to hollow beam-like structures: 1) CA provides an estimate of axial compressive or tensile strength; 2) J is an estimate of average torsional and bending rigidity; and 3) Imax:Imin ratio provides information about the cross-sectional shape and distribution of the material (Ruff, 1981, 1989; Ruff and Hayes, 1983; Swartz et al., 1992; Heinrich et al., 1999).

Section modulus (Z). The cross-sectional strength of a bone can be characterized as the bending or torsional moment required to cause fracture. These ultimate moments are approximately proportional to the ratio, Z, which can be calculated from the dimensions of the section (van der Meulen et al., 1996; Alexander, 1998):

$$Z = J/D$$

where J is the polar moment of inertia and D is the mean diameter of the cross-section (Heinrich et al., 1999, and pers. commun.).

Statistical/Data Analysis; Allometric Analysis

Means and percentages are reported with ±1 SD. Unless otherwise stated, percent differences were calculated with reference to datasets from the cranial, lateral, or combined medial and lateral cortices. For example: [((cranial-caudal)/cranial) · 100], or [((medial-lateral)/lateral) · 100].

Normality testing revealed that 13.5% of microstructure data subsets and 11% of geometry data subsets were not normally distributed. Examination of these subsets showed that few of these datasets were J-shaped or severely skewed, which we defined as a skewness value >1.0 or <–1.0. According to Kachigan (1986), parametric tests are more powerful in this situation than the alternative nonparametric test provided that a *P*-value of <0.01 is used for the nonnormally distributed datasets. Thus, we report results of parametric testing using a one-way analysis of variance (ANOVA) and Fisher's LSD post-hoc test using the standard *P*-value of <0.05 for statistical significance, and $P < 0.01$ for nonnormally distributed datasets. Data were fit to linear equations using the least-squares line-fitting technique. Nonlinear equations were used where appropriate. The nonlinear equations selected exhibited superior goodness-of-fit when compared to other regression equations (TableCurve v. 4.00, Jandel Scientific, San Rafael, CA). Regression coefficients and *P*-values were obtained using a commercially available statistical program (StatView v. 5.0, SAS Institute, Cary, NC).

The magnitudes of the correlation coefficients (r) were interpreted according to the classification of Hinkle et al. (1979, p. 85). In this scheme, coefficients in the ranges of 0.9–0.99, 0.7–0.89, 0.5–0.69, 0.3–0.49, and 0.0–0.29 are interpreted, respectively, as representing very high, high, moderate, low, and little if any correlation.

Scaling relationships of length vs. geometric parameters. A bone that scales geometrically maintains a constant shape as it increases in size. For example, geometric scaling of a bone occurs when the volume enclosed by the periosteum and cartilage changes in proportion to its $(\text{length})^3$. Allometric scaling occurs when a bone changes with different rates in both size and shape. Allometric scaling is estimated by the equation $y = ax^b$ where y is the parameter being examined in relation to body mass or bone length; x is bone length (typically strongly correlated with body mass); and b is the scaling exponent that corresponds to the slope of the linear plot of log-transformed data represented by the equation $\log(y) = \log(a) + b \cdot \log(x)$ (Swartz and Biewener, 1992).

Regression analyses were conducted for length vs. each of the cross-sectional measurements and geometric properties using: 1) all bones, 2) adults and subadults, and 3) young and old fawns. Reduced major axis (RMA) regression, which assumes that errors are evenly partitioned between the x and y variables, was used to estimate b (Rayner, 1985; Heinrich et al., 1999). RMA is the most appropriate line-fitting technique when error variances of the two variables are unknown and correlated (Rayner, 1985). The reduced major axis slope b is equal to the least squares slope divided by the correlation coefficient (r).

RESULTS

Material Characteristics

General histology: age-related changes and regional differences (Fig. 2). Primary woven bone with trabecular structure was prevalent in fetal and young fawn bones. Older fawns exhibited increased prevalence of simple primary osteonal bone (Stover et al., 1992) with occasional secondary osteons. Subadult bones demonstrate plexiform or simple primary osteonal bone on the periosteal surfaces and an abundance of secondary osteons in the subjacent tissue. In subadult bones, circumferential lamellar bone, when present, appeared on the periosteal surfaces of the medial and lateral cortices. When viewing both subadult and adult bones in circularly polarized light, secondary osteons in the cranial and medial cortices were primarily of the lamellar type (table II in Marotti, 1996). In these age groups, secondary osteons in the caudal and lateral cortices were primarily of the parallel-fibered type (Marotti, 1996) (G. Marotti viewed our images and agreed with these general distinctions). In adult bones, a thin layer of circumferential lamellar bone (Stover et al., 1992) was present on the periosteal surface in all locations.

Mineral content (% ash) (Table 4; Figs. 3a, 4). The caudal (i.e., "tension") cortex has lower average mineral content than all other cortices in all age groups. This is statistically significant ($P < 0.05$) in nearly all cortical comparisons—except for caudal vs. medial in young fawns ($P > 0.5$). The cranial cortex consistently shows the highest mineral content. There is little change in the cranial:caudal % ash ratio with age ($P > 0.5$). This represents a 4% relative (2.5% absolute) cranial vs. caudal difference in the young fawns, and a 6.6% relative (4.3% absolute) difference in each of the other groups. Cranial % ash was invariably *greater* than caudal % ash in *all bones* from older fawn, subadult, and adult age groups. The average % ash of the cranial cortex in adult specimens is 10% greater (6.9% absolute difference) than the cranial cortex of younger fawns (64.6 ± 3.8 vs. 71.5 ± 2.3, $P < 0.001$). However, the two fetal bones showed lower % ash in the *cranial* cortex when compared to the caudal cortex (cranial vs. caudal: 61.6% vs. 62.1%, 64.5% vs. 65.3%). As described below, this is most likely a consequence of residual calcified cartilage in the caudal cortices of these specimens. There were no significant % ash differences between medial and lateral comparisons in *any* age group.

The fetal bones and several young fawn bones showed evidence of highly mineralized tissue consistent with residual calcified cartilage from the resorbing cartilaginous anlagen. In the two young fawns that demonstrated a greater caudal % ash relative to cranial % ash, this hypermineralized tissue was found in all images taken from the caudal cortex, 75% of images taken from the lateral cortex, and in more than half of the images from cranial and medial cortices. In the caudal cortex images of these two bones, up to 20–25% of the bone material displayed this hypermineralized tissue compared with 10–15% of bone material in cranial cortex images. These observations support the possibility that the increased % ash in the caudal cortex relative to the cranial cortex in these

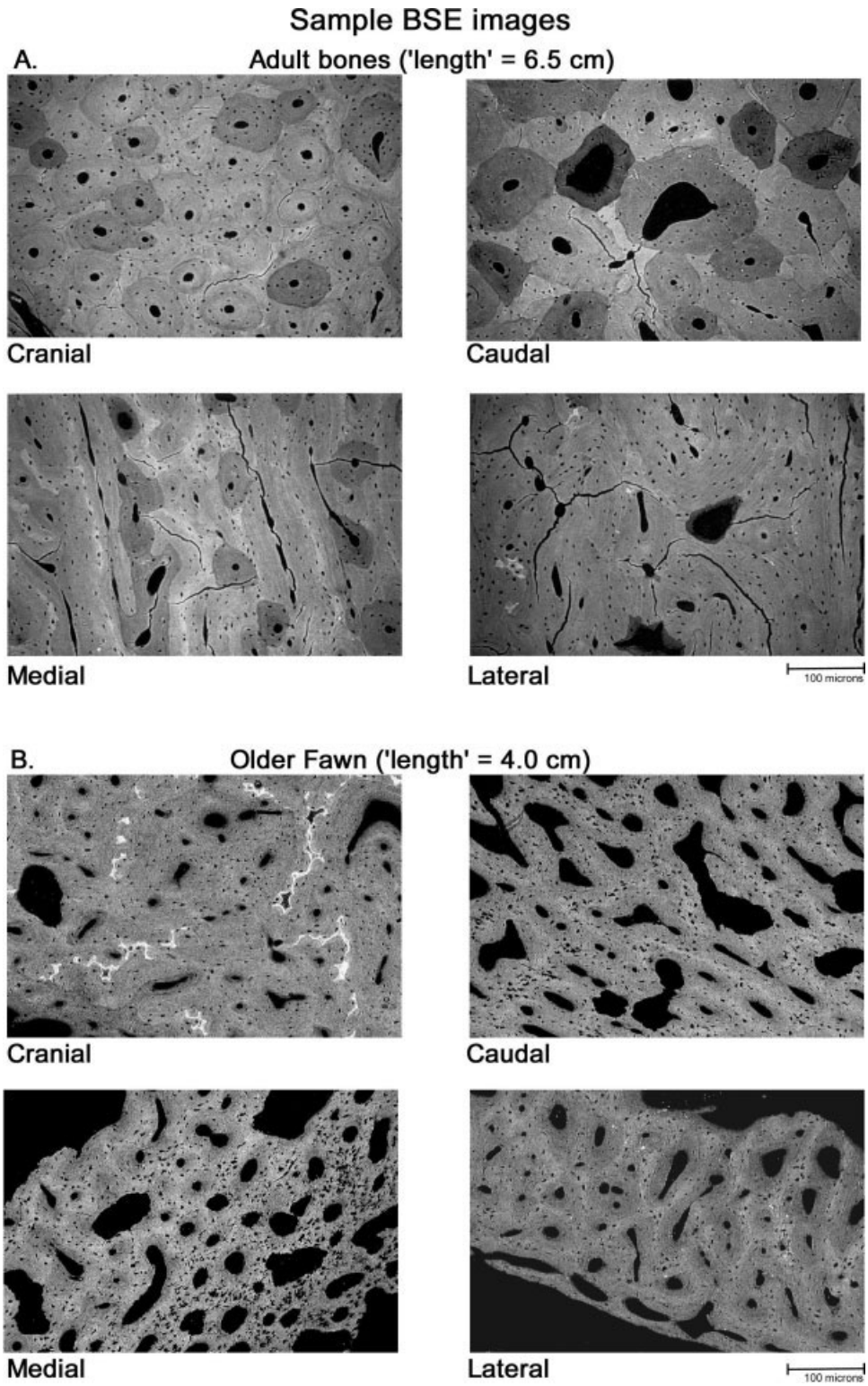

Fig. 2. Representative backscattered electron images from all four cortices of: (**A**) an adult specimen, and (**B**) an older fawn specimen. Note that the cranial cortex of adult bones shows a greater number of secondary osteons with a smaller average cross-sectional area compared to osteons in the caudal cortex. The medial and lateral cortices of the adult specimen show relatively more prevalent elliptically shaped osteons. See the Discussion section for a description of the histology of each age group.

two atypical bones may be due to calcified cartilage.

Porosity (Po/Ar) (Table 4; Fig. 3b). Mean percent porosity in cortical bone decreases with age. Porosity variations between individual cortical locations remain roughly uniform until the subadult and adult age groups, wherein the caudal cortex exhibits significantly higher porosity compared to the other cortices ($P < 0.05$). Specifically, in subadult specimens, the average absolute porosity difference be-

*TABLE 4. Microstructure, CFO, and % ash content**

Cortical region	% Ash Mean SD	Po/Ar Mean SD	N.On/Ar Mean SD	On.B/Ar Mean SD	NREs Mean SD	N.Lac/Ar Mean SD	CFO Mean SD
Young fawn (n = 9)							
Cranial	64.6 ± 3.8	54.6 ± 11.1	0.1 ± 0.1	1.7 ± 7.8[a]	0.1 ± 0.1	343.0 ± 89.5	126.1 ± 19.0
Caudal	62.1 ± 4.8	51.3 ± 18.8	0.0 ± 0.0	0.0 ± 0.0	0.0 ± 0.0	365.0 ± 60.8	114.3 ± 32.6
Medial	62.2 ± 5.5	60.5 ± 15.3	0.0 ± 0.0	0.0 ± 0.0	0.0 ± 0.0	341.3 ± 68.3	128.3 ± 16.9[b]
Lateral	64.9 ± 4.7	69.4 ± 28.6	0.0 ± 0.0	0.0 ± 0.0	0.0 ± 0.0	368.6 ± 57.4	89.1 ± 19.0
All regions	63.4 ± 4.7	58.8 ± 20.4	0.0 ± 0.0	0.1 ± 0.6	0.0 ± 0.0	354.8 ± 69.6	114.4 ± 32.4
Older fawn (n = 6)							
Cranial	69.6 ± 2.0[a]	17.7 ± 8.4[a]	1.6 ± 0.4	4.3 ± 1.1	2.9 ± 0.5	575.3 ± 98.4	104.4 ± 25.6
Caudal	65.3 ± 3.6	32.3 ± 13.3	0.6 ± 0.2	2.3 ± 2.0	2.3 ± 0.7	590.7 ± 135.4	116.5 ± 33.9
Medial	67.7 ± 2.0	25.2 ± 12.6	0.8 ± 0.3	2.9 ± 0.9	2.0 ± 0.4[b]	507.7 ± 91.9	115.8 ± 26.5
Lateral	66.6 ± 3.1	31.4 ± 17.5	0.3 ± 0.2	1.1 ± 0.5	0.9 ± 0.4	513.9 ± 93.2	125.8 ± 26.5
All regions	67.3 ± 2.7	25.9 ± 13.9	0.9 ± 0.2	3.2 ± 0.6	2.0 ± 3.5	559.8 ± 114.6	115.6 ± 25.4
Subadult (n = 11)							
Cranial	69.7 ± 4.6[a]	7.9 ± 4.1[a]	19.3 ± 2.2[a]	35.8 ± 4.0[a]	2.2 ± 0.4[a]	594.4 ± 65.1	98.3 ± 23.9
Caudal	65.4 ± 3.6	17.1 ± 9.6	16.9 ± 2.0	42.0 ± 5.3	4.2 ± 0.3	556.7 ± 128.0	81.1 ± 12.9
Medial	67.8 ± 5.4	6.4 ± 1.1	9.4 ± 2.6	23.2 ± 6.0	1.4 ± 0.3	522.5 ± 47.5	119.5 ± 23.0
Lateral	67.7 ± 4.9	6.3 ± 1.2	8.6 ± 2.8	23.8 ± 5.0	1.2 ± 0.3	532.5 ± 65.2	106.1 ± 36.8
All regions	67.7 ± 4.6	10.8 ± 8.2	15.4 ± 1.7	34.8 ± 2.7	2.3 ± 0.4	562.8 ± 94.2	101.2 ± 27.8
Adult (n = 10)							
Cranial	71.5 ± 2.3[a]	4.6 ± 1.9[a]	37.7 ± 15.2[a]	56.9 ± 20.5[a]	1.1 ± 0.2[a]	538.4 ± 69.3[a]	88.4 ± 18.7[a]
Caudal	67.1 ± 4.9	9.3 ± 6.1	33.2 ± 10.0	76.6 ± 13.1	2.3 ± 0.3	417.8 ± 74.8	63.3 ± 10.6
Medial	70.5 ± 2.0	2.5 ± 1.2	22.0 ± 8.8	32.3 ± 13.1	0.7 ± 0.2	454.5 ± 39.9	110.7 ± 24.9
Lateral	71.1 ± 2.0	2.6 ± 1.9	13.3 ± 6.4	24.6 ± 12.2	0.6 ± 0.2	451.8 ± 42.2	102.1 ± 23.1
All regions	70.1 ± 2.8	5.8 ± 4.8	26.5 ± 8.4	56.7 ± 24.7	1.2 ± 2.4	465.6 ± 52.3	91.1 ± 26.2

Mean values ± standard deviations.
*See Table 3 for abbreviations.
[a]Statistically significant cranial–caudal difference ($P < 0.01$).
[b]Statistically significant medial–lateral difference ($P < 0.05$).

tween caudal and all other cortices is 10.2% ($P < 0.001$); in adult specimens the difference between caudal and all other cortices is 6.0% ($P < 0.001$). There were no significant differences in Po/Ar between medial and lateral cortices in all age groups ($P > 0.3$).

Secondary osteon population density (N.On/Ar) and fractional area of secondary bone (On.B/Ar) (Table 4; Fig. 3c,d). Secondary osteons were rarely present in younger fawns (Cranial cortex: <1.0 per mm^2). Each of the other age groups showed significantly more osteons in the cranial cortex compared to the other three cortices ($P < 0.01$). There were no significant differences in N.On/Ar or On.B/Ar between medial and lateral cortices in all age groups ($P > 0.3$). On.B/Ar data in subadults and adults show a relatively greater percentage of secondary bone in the caudal cortex compared to the cranial cortex. These data are consistent with our observations that secondary osteons have relatively smaller cross-sectional areas in the cranial cortex.

New remodeling events (NREs) (Table 4; Fig. 3e). Aside from rare occurrences in the cranial cortex (<1.0 per mm^2), NREs were not present in younger fawns. In the older fawn group, cranial and caudal cortices contain more NREs than the other cortices, although this is only statistically significant in comparison with the lateral cortex ($P < 0.05$). The caudal cortex contains a greater number of NREs in both subadults ($P < 0.01$) and adults ($P < 0.01$) compared to the cranial cortex. In both adults and subadults, the caudal cortex has significantly more NREs than medial and lateral cortices ($P < 0.05$).

Osteocyte lacuna population density (N.Lac/Ar) (Table 4; Fig. 3f). There are fewer osteocyte lacunae in young fawns when compared to all other groups ($P < 0.001$). In adult bones, the cranial cortex has the greatest N.Lac/Ar. The cranial cortex also contains significantly more lacunae than medial and lateral cortices in older fawns and subadults ($P < 0.05$), but is similar to the caudal cortex in these groups. There were no significant differences in N.Lac/Ar between medial and lateral cortices in any age group. The adult bones contained significantly fewer osteocyte lacunae when compared with subadults and older fawns ($P < 0.001$).

Predominant collagen fiber orientation (CFO; expressed as weighted mean graylevel (WMGL)) (Tables 4, 5a; Fig. 5a,b). Fetal bones, young fawns, and older fawns demonstrated inconsistent regional CFO variations. Consistent differences between the cranial and caudal cortices begin to emerge by the subadult age group (length ~5.6 cm) and are statistically significant in adult bones ($P < 0.05$). Medial-to-lateral comparisons showed significant CFO anisotropy only in younger fawns; all other age groups showed no differences between medial and lateral cortices. When data from all bones and all cortices are considered, correlation analysis demonstrated low negative correlation between CFO and N.On/Ar (–0.449, $P < 0.01$) and

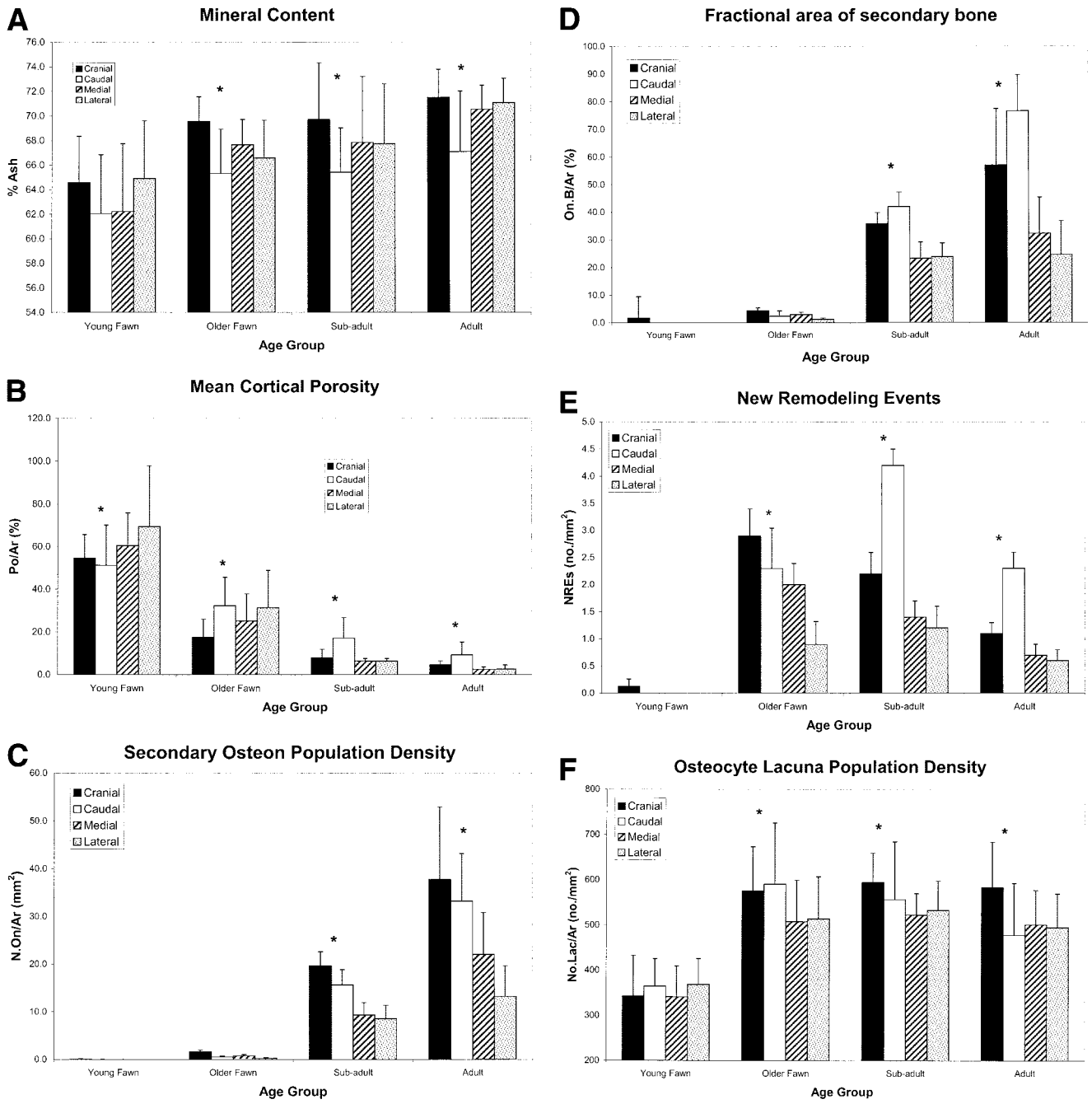

Fig. 3. Microstructure and mineral content. *$P < 0.05$ for cranial vs. caudal comparisons. **A:** % Ash. In young fawns, the caudal cortex tended toward lower % ash content than the cranial cortex ($P = 0.068$). However, when only the two fetal bones were examined, the caudal cortex had significantly higher % ash compared to the cranial cortex ($P < 0.05$). In older fawns, subadults, and adults, the cranial cortex had significantly greater % ash than the caudal cortex ($P < 0.05$). There were no significant differences in % ash between medial and lateral cortices in any age group. **B:** Porosity. In young fawns, Po/Ar is greater in the lateral cortex (a tension/shear region) compared to the cranial and caudal cortices ($P < 0.05$). In older fawns, the lateral cortex has greater porosity than medial and cranial ($P < 0.05$) and the cranial cortex has a lower porosity than all other cortices ($P < 0.05$). In subadults, the caudal cortex has a greater porosity compared to the other cortices ($P < 0.01$). In adult bones, both cranial and caudal cortices have greater porosity compared to medial and lateral cortices ($P < 0.05$), and the caudal cortex is more porous than the cranial ($P < 0.05$). **C:** N.On/Ar. In subadults and adults, the cranial and caudal cortices have significantly higher N.On/Ar than medial and lateral cortices ($P < 0.05$), with the cranial cortex being significantly higher than the caudal cortex ($P < 0.05$). There were no significant differences between medial and lateral cortices in any age group. **D:** On.B/Ar. In subadults and adults, cranial and caudal cortices have significantly higher On.B/Ar than medial and lateral cortices ($P < 0.01$). The caudal cortex has higher On.B/Ar than the cranial cortex only in subadults ($P < 0.01$) and adults ($P < 0.01$). There were no significant differences between medial and lateral cortices in any age group. **E:** NREs. In young fawns, no NREs were seen in caudal, medial or lateral cortices. In subadults and adults, the caudal cortex contained significantly more NREs compared to the cranial, medial, and lateral cortices. ($P < 0.01$). *$P < 0.01$ for cranial vs. caudal comparison. **F:** N.Lac/Ar. In young fawns, there are no significant N.Lac/Ar differences. In older fawns, both cranial and caudal cortices have significantly more lacunae per area than the medial and lateral cortices ($P < 0.05$). In subadults, the cranial cortex has significantly more lacunae than the medial and lateral cortices ($P < 0.05$). In adult bones, the cranial cortex has significantly more lacunae per area than other cortices ($P < 0.001$).

*TABLE 5A. Correlations: microstructure in all calcanei (r values)**

All cortices	Po/Ar	N.Lac/Ar	CFO*	N.On/Ar	On.B/Ar	NREs	% Ash*	Lng (cm)	Ct.Th
Po/Ar	1.000								
N.Lac/Ar	−0.596[c]	1.000							
CFO	0.155	−0.132	1.000						
N.On/Ar	−0.566[c]	0.200[a]	−0.449[c]	1.000					
On.B/Ar	−0.579[c]	0.169	−0.502[c]	0.876[c]	1.000				
NREs	−0.173	0.229[c]	−0.399[c]	0.066	0.191	1.000			
% Ash	−0.618	0.300	0.138	0.181	0.142	0.320[b]	1.000		
Lng (cm)	−0.853[c]	0.377[b]	−0.377[c]	0.697[c]	0.767[c]	0.145	0.457[a]	1.000	
Ct.Th	−0.530[c]	0.449[c]	−0.108	0.673[c]	0.649[c]	0.454[b]	0.398[c]	0.614[c]	1.000
Cranial	**Po/Ar**	**N.Lac/Ar**	**CFO***	**N.On/Ar**	**On.B/Ar**	**NREs**	**% Ash***	**Lng (cm)**	**Ct.Th**
Po/Ar	1.000								
N.Lac/Ar	−0.675[c]	1.000							
CFO	0.386	−0.359	1.000						
N.On/Ar	−0.541[c]	0.319[a]	−0.404	1.000					
On.B/Ar	−0.612[c]	0.214[a]	−0.447[a]	0.869[c]	1.000				
NREs	−0.101	0.137	−0.369	−0.133	−0.134	1.000			
% Ash	−0.719[c]	0.564[b]	−0.025	0.140	0.156	0.389[a]	1.000		
Lng (cm)	−0.876[c]	0.474[a]	−0.458[a]	0.688[c]	0.798[c]	−0.081	0.770[a]	1.000	
Ct.Th	−0.792[c]	0.445[a]	−0.273	0.813[c]	0.884[c]	0.357	0.714[c]	0.955[c]	1.000
Caudal	**Po/Ar**	**N.Lac/Ar**	**CFO***	**N.On/Ar**	**On.B/Ar**	**NREs**	**% Ash***	**Lng (cm)**	**Ct.Th**
Po/Ar	1.000								
N.Lac/Ar	−0.209	1.000							
CFO	0.448[a]	0.073	1.000						
N.On/Ar	−0.737[c]	−0.128	−0.622[c]	1.000					
On.B/Ar	−0.770[c]	−0.146	−0.635[c]	0.887[c]	1.000				
NREs	−0.212	0.263[b]	−0.604[c]	0.113	0.227	1.000			
% Ash	−0.710[c]	0.347[b]	0.234	−0.004	0.060	0.293	1.000		
Lng (cm)	−0.845[c]	0.096	−0.624[c]	0.781[c]	0.896[c]	0.233	0.504[b]	1.000	
Ct.Th	−0.587[c]	0.635[c]	−0.154	0.336	0.459[b]	0.742[c]	0.668[c]	0.714[c]	1.000

[a]$P < 0.05$.
[b]$P < 0.01$.
[c]$P < 0.001$.
Lng = bone length; Ct.Th = cortical thickness; see Table 3 for abbreviations.
*Data for correlations for all charactersitics except for CFO and % ash included all animals (n = 36). Data for CFO correlations was obtained from a subset (n = 21) of animals. Data for % ash correlations was obtained from a different subset (n = 15) of animals that partially overlapped (n = 12) the CFO subset.

moderate negative correlation of CFO between CFO and On.B/Ar (r = −0.502, $P < 0.01$) (Table 5a). Correlation analysis of the caudal cortex alone showed a stronger moderate correlation of CFO with both N.On/Ar (r = −0.622, $P < 0.001$) and On.B/Ar (r = −0.635, $P < 0.001$). Analysis of the cranial cortex alone showed low negative correlation of CFO with both N.On/Ar (r = −0.404, $P < 0.01$) and On.B/Ar (r = −0.447, $P < 0.01$).

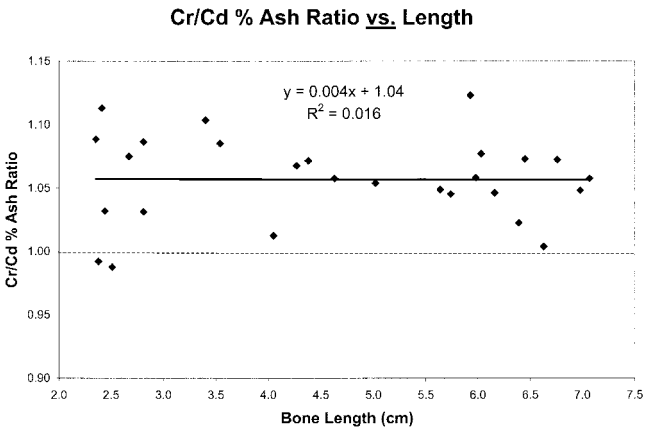

Fig. 4. Cr/Cd % ash ratio vs. length. This plot shows the flat linear relationship of Cranial:Caudal % ash ratio. Note that all specimens have a ratio >1.0 except for two younger fawns.

Structural Characteristics

Cross-sectional shape, cortical area, and cortical thickness (Table 6; Figs. 6–8). The calcaneus exhibits greater expansion in the cranial–caudal direction than in the medial–lateral direction, with the height:width ratio increasing linearly relative to bone length (Figs. 6, 7, r = 0.922, $P < 0.001$). Both cortical area (CA) and total area (TA) progressively increase with bone length (Fig. 8a). There is a small linear increase in CA:TA ratio with increasing length (r = 0.725, $P < 0.001$). The Imax:Imin ratio increased linearly with length (r = 0.908, $P < 0.001$), while Imax and polar moment of inertia (J, mm^4) increased exponentially (Fig. 8b,c)

*TABLE 5B. Correlations: microstructure, CFO, and cortical thickness (r values)**

All cortices	Po/Ar	N.Lac/Ar	CFO*	N.On/Ar	On.B/Ar	NREs	% Ash*	Lng (cm)	Ct.Th	
Po/Ar	1.000	−0.024	−0.370[a]	−0.352[b]	−0.107	0.519[c]	−0.468[a]	−0.582[c]	−0.095	
N.Lac/Ar	−0.582[c]	1.000	0.132	0.005	−0.260[a]	0.041	−0.035	−0.263[b]	0.210	
CFO	−0.167	−0.109	1.000	−0.374[a]	−0.516[c]	−0.470[a]	0.774[b]	0.153	−0.105	
N.On/Ar	−0.363[a]	0.245	−0.046	1.000	0.752[c]	−0.111	0.057	0.458[c]	0.570[c]	
On.B/Ar	−0.323[c]	0.276	−0.034	0.847[c]	1.000	0.016	−0.267	0.533[c]	0.505[c]	
NREs	−0.433[c]	0.428[c]	−0.076	0.742[c]	0.847[c]	1.000	−0.613[b]	−0.464[b]	0.191	
% Ash	−0.559[c]	0.305[c]	0.253[a]	0.235[b]	0.197	0.288[b]	1.000	0.271	0.064	
Lng (cm)	−0.700[c]	0.782[c]	−0.097	0.378[b]	0.364[c]	0.521[c]	0.344[a]	1.000	.0300[a]	
Ct.Th	−0.466[c]	0.522[c]	0.088	0.096	0.150	0.323[b]	0.322[b]	0.487[c]	1.000	

←Fawns Only→ ←Sub-adults&Adults→

Cranial	Po/Ar	N.Lac/Ar	CFO*	N.On/Ar	On.B/Ar	NREs	% Ash*	Lng (cm)	Ct.Th	
Po/Ar	1.000	−0.094	0.100	−0.394[b]	−0.406[a]	0.655[a]	0.022	−0.686[c]	−0.801[c]	
N.Lac/Ar	−0.737[c]	1.000	0.181	0.163	−0.140	−0.029	−0.323	−0.102	−0.183	
CFO	−0.086	−0.327	1.000	−0.333	−0.498	−0.209	0.981[c]	−0.378	−0.291	
N.On/Ar	−0.419[a]	0.209	−0.247	1.000	0.770[c]	−0.244	−0.424	0.459[c]	0.847[c]	
On.B/Ar	−0.392[b]	0.208	−0.196	0.924[c]	1.000	−0.581[a]	−0.534	0.655[c]	0.843[c]	
NREs	−0.550[b]	0.407[a]	−0.252	0.825[c]	0.756[c]	1.000	−0.806[a]	−0.644[a]	−0.451	
% Ash	−0.661[b]	0.642[a]	0.087	0.236	0.178	0.443	1.000	0.346	0.991[c]	
Lng (cm)	−0.854[c]	0.806[c]	−0.364	0.423[a]	0.381[a]	0.582[c]	0.779[b]	1.000	0.945[c]	
Ct.Th	−0.811[c]	0.757[c]	−0.283	0.259	0.245	0.540[a]	0.654[b]	0.907[c]	1.000	

←Fawns Only→ ←Sub-adults&Adults→

Caudal	Po/Ar	N.Lac/Ar	CFO*	N.On/Ar	On.B/Ar	NREs	% Ash*	Lng (cm)	Ct.Th	
Po/Ar	1.000	0.159	0.322	−0.760[c]	−0.643[c]	0.518[a]	0.095	−0.754[c]	0.335	
N.Lac/Ar	−0.595[a]	1.000	0.594	−0.327	−0.532[b]	0.210	−0.174	−0.764[c]	0.375	
CFO	−0.086	0.011	1.000	−0.598	−0.669[a]	−0.724[b]	0.975[c]	−0.298	0.020	
N.On/Ar	−0.234	0.163	−0.184	1.000	0.763[c]	−0.165	−0.548	0.623[c]	−0.212	
On.B/Ar	−0.286	0.264	−0.222	0.935[c]	1.000	−0.109	−0.769[a]	0.816[c]	−0.077	
NREs	−0.360	0.367[a]	−0.151	0.811[c]	0.926[c]	1.000	−0.897[b]	−0.417[a]	0.661[b]	
% Ash	−0.738[c]	0.427[a]	0.459	0.034	0.093	0.238	1.000	0.123	−0.738[b]	
Lng (cm)	−0.568[a]	0.769[c]	−0.087	0.311	0.364[a]	0.464[b]	0.419[a]	1.000	−0.553[a]	
Ct.Th	−0.421	0.774[c]	0.185	0.304	0.603[b]	0.652[b]	0.673[b]	0.863[c]	1.000	

←Fawns Only→ ←Sub-adults&Adults→

[a]$P < 0.05$.
[b]$P < 0.01$.
[c]$P < 0.001$.
Lng, bone length in cm; Ct.Th = cortical thickness; see Table 3 for abbreviations.
*Within each matrix, lower left values represent all fawns, upper right values represent adults and subadults. Data for correlations for all charactersitics except for WMGL and % ash included all specimens (n = 36). Data for WMGL correlations were obtained from a subset (n = 21) of specimens. Data for % ash correlations were obtained from a different subset (n = 15) of specimens that partially overlapped (n = 12) the WMGL subset.

(Imax: b = 0.970, r = 0.985, $P < 0.001$; J: b = 0.767, r = 0.922, $P < 0.001$).

Relative to the caudal cortex, the cranial cortex increases in thickness in an exponential fashion (b = 0.300, r = 0.911, $P < 0.001$), with the greatest difference occurring between older fawns and subadults (Fig. 7c; Table 6). While the cranial cortex increases in thickness by a factor of 4 (1.2 mm in young fawns to 8.4 mm in adults), the caudal, medial, and lateral cortices increase by a factor of about 2–21/2 (caudal cortex: 1.8–4.0 mm; medial cortex: 1.1–2.6 mm, lateral cortex: 0.7–2.6 mm; Fig. 7; Table 6). As a percentage of total subperiosteal cranial–caudal "height," the cranial cortex triples (11.4% in young fawns to 34.2% in adults) while the caudal cortex increases in older fawns then decreases in adults (18.2–16.6%) (Fig. 7b). The increased porosity observed along the endosteal caudal cortex in older fawns, which may represent the formation of cancellous bone, accounts for the subsequent decrease in caudal cortical thickness seen in subadult and adult specimens (Fig. 6).

Trabecular bone patterns. Examination of lateral radiographs of *fetal* bones revealed the unmistakable presence of arched trabecular patterns. These patterns are grossly similar to those seen in bones of all other age groups.

Additional Regression Analysis

Regressions: all bones (Table 5a). Some regression results are reported in the preceding two sections. When all bones and all cortices are considered, analysis of growth-related microstructural variations reveal a moderate positive correlation between bone length and N.On/Ar (r = 0.697, $P < 0.001$) and a low positive correlation between bone length and N.Lac/Ar (r = 0.377, $P < 0.001$). Moderate positive correlations were found between bone length and the ratio of Cr:Cd N.On/Ar (r = 0.609,

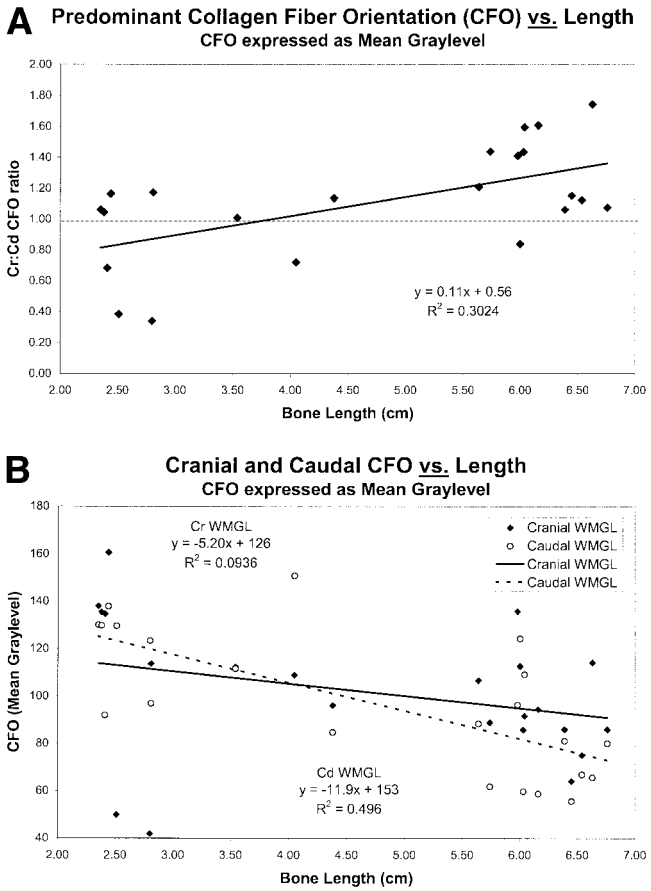

Fig. 5. Predominant collagen fiber orientation (CFO). **A:** Cranial:Caudal CFO ratio vs. bone length. **B:** Linear plot showing cranial CFO and caudal CFO vs. bone length. Note that there is an overall decline in both cranial and caudal cortices, but the caudal cortex decreases in a more dramatic fashion than the cranial cortex.

$P < 0.001$) as well as the ratio of Cr:Cd N.Lac/Ar ($r = 0.652$, $P < 0.001$). From subadults to adults, this demonstrates progressively more secondary osteons in the cranial cortex compared to the caudal cortex (Fig. 9a). There was no correlation between bone length and Cr:Cd % ash ratio ($r = 0.126$, $P = 0.52$). There was a low positive correlation between Cr:Cd N.On/Ar and Cr:Cd N.Lac/Ar ($r = 0.429$, $P < 0.01$).

Linear regressions of all cortices in all bones demonstrated a moderate positive correlation between bone length and % ash ($r = 0.457$, $P < 0.05$). Bone length vs. % ash exhibited a positive correlation in each individual cortex ($r = 0.770$, 0.504, 0.620, and 0.444, respectively, for cranial, caudal, medial, and lateral cortices, $P < 0.05$).

There were very high positive correlations between bone length and cortical area ($r = 0.965$, $P < 0.001$), total area ($r = 0.963$, $P < 0.001$), and Imax:Imin ratio ($r = 0.951$, $P < 0.001$), and a high positive correlation between bone length and cortical area to total area (CA:TA) ratio ($r = 0.787$, $P < 0.001$).

Segregated regressions: fawns only; subadults and adults only (Table 5b). When fawns were independently examined, bone length showed a high negative correlation with Po/Ar ($r = -0.700$, $P < 0.001$) and a high positive correlation with N.Lac/Ar ($r = 0.782$, $P < 0.001$). Results of other correlation analyses of segregated groups are shown in Table 5b.

Allometric regressions (Table 7; Figs. 7, 8). Selected allometric regressions are shown in Figures 7 and 8. In all cases reduced mean axis (RMA) analysis showed high to very high positive correlations (all with $r > 0.800$, $P < 0.001$). When all age groups were included, all geometric characteristics exhibited negative allometry vs. bone length, as indicated by 95% confidence intervals being below isometry. These negative allometries are most notable along the medial–lateral axis (Imin and "width"). Stratified analysis of subadult and adult bones showed isometry for height, width, cortical area, section modulus, and Imax; all other characteristics exhibited negative allometries. When examined alone, the fawn groups similarly showed isometry for height, section modulus, and Imax, with negative allometries for all other characteristics. No scaling exponents significantly exceeded the predicted isometry.

DISCUSSION

Some of the regional structural and material cortical variations in the mule deer calcaneus may represent important adaptations. The possibility that they are "strain-mode-specific" is suggested by data showing that mechanical properties and fracture and microdamage mechanics of cortical bone markedly differ in tension, compression, and shear loading modes (Burstein et al., 1972, 1976; Reilly and Burstein, 1974, 1975; Carter and Hayes, 1977; Norman et al., 1995, 1996; Pattin et al., 1996; Burr et al., 1998; Huja et al., 1999; Reilly and Currey, 1999, 2000; Turner et al., 2001). Variations in strain magnitudes, which are highest in the cranial cortex, and principal strain directions, which are most oblique in the medial and lateral cortices, may also be important mediators of some morphologic characteristics (Su et al., 1999). However, some characteristics may be controlled and constrained by genetic and epigenetic influences, including positional information (see below). These influences may be most important during earlier phases of ontogeny, with the effects of extragenetic stimuli (e.g., microdamage events) subsequently becoming more important. These possibilities are suggested by several exceptions to our predicted structural and material changes (Table 1), including: 1) arched trabecular patterns *are recognizable* in the fetal bones; 2) fetal and young fawn bones *are not* circular in cross section, but are quasi-circular to quasi-elliptical with the ma-

TABLE 6. Cortical thickness and geometry of deer calcanei Mean values and (standard deviations).

A. Cortical Thickness and Cross-Sectional Diameter Data (in mm)

Group age	Ht	Wd	Cr	Cd	Med	Lat	Cr/Cd	Cr/Ht	Cd/Ht	Med/Wd	Lat/Wd
Young fawn	10.2[a]	7.2	1.2	1.8	1.1	0.7	0.65	11.4[a]	18.2	15.2[a]	10.6
	(1.0)	(1.2)	(0.3)	(0.5)	(0.4)	(0.2)	(0.1)	(0.03)	(0.06)	(0.07)	(0.04)
Older fawn	16.3[a]	8.6	3.1[a]	4.2	1.4	1.2	0.75	18.9[a]	25.5	16.4[a]	14.2
	(1.8)	(0.6)	(0.6)	(1.1)	(0.2)	(0.3)	(0.1)	(0.02)	(0.04)	(0.03)	(0.04)
Subadult	21.4[a]	9.1	6.1[a]	4.5	2.1	2.1	1.38	28.2[a]	21.2	22.7	22.9
	(1.3)	(0.9)	(1.6)	(0.8)	(0.6)	(0.6)	(0.4)	(0.06)	(0.04)	(0.06)	(0.06)
Adult	24.2[a]	10.0	8.4[a]	4.0	2.6	2.6	2.13	34.2[a]	16.6	26.7	26.2
	(1.3)	(0.7)	(1.2)	(0.8)	(0.3)	(0.2)	(0.5)	(0.04)	(0.03)	(0.02)	(0.02)
P value	<0.001	<0.001	<0.001	<0.001	<0.001	<0.001	<0.001	<0.001	0.0046	<0.001	<0.001

B. Geometry data (areas in mm^2; moments in mm^4; Z in mm^3)

Group age	CA	TA	CA/TA	Imax	Imin	Imax/Imin	J	Z
Young fawn	37.36	57.02	0.67	324.2	176.0	1.96	500.2	55.80
	(7.8)	(16.1)	(0.1)	(145.9)	(97.6)	(0.30)	(242.5)	(20.4)
Older fawn	84.65	120.83	0.69	1941.8	608.7	3.17	2550.6	200.38
	(18.3)	(20.7)	(0.1)	(691.4)	(189.)	(0.42)	(866.8)	(64.4)
Subadult	135.72	172.68	0.78	4895.4	1134.9	4.35	6030.3	433.44
	(26.1)	(24.4)	(0.1)	(1450.9)	(353.4)	(0.49)	(1784.5)	(102.4)
Adult	178.84	221.70	0.81	8717.3	1752.4	5.03	10469.6	626.55
	(15.3)	(19.0)	(0.0)	(1563.8)	(325.9)	(0.72)	(1809.4)	(105.8)
P value	<0.001	<0.001	<0.001	<0.001	<0.001	<0.001	<0.001	<0.001

A: Ht, cranial-caudal subperiosteal 'height'; Wd, medial-lateral subperiosteal 'width'; Cr, cranial; Cd, caudal; Med, medial; Lat, lateral; Cr/Cd is expressed as a ratio; All other ratios are expressed as percents.
B: CA/TA is expressed as a ratio; See Table 3 for abbreviations.
P value = represents comparison between four groups.
[a]Statistically significant ($P = 0.05$) *within* group differences in Ht *vs.* Wd, Cr *vs.* Cd, Med *vs.* Lat, Cr/Ht *vs.* Cd/Ht, and/or Med/Wd *vs.* Lat/Wd.

jor axis in the cranial–caudal direction of predominant bending; 3) there is a period of time when the caudal cortex of young fawns (excluding fetal bones) *exceeded the thickness of the cranial cortex;* and 4) % ash is *not* uniform (e.g., cranial > caudal) in most fetal and young fawn bones.

Biomechanical Relevance of Material Variations

Whole-bone mineral content. An ontogenetic increase in a bone's ability to withstand stress through structural and/or material modifications has been reported in various species, with these studies typically focusing on cross-sectional geometry and/or mineral content (Currey and Butler, 1975; Torzilli et al., 1981; Carrier, 1983; Keller et al., 1985; Schaffler and Burr, 1988; Currey and Pond, 1989; Carrier and Leon, 1990; Brear et al., 1990; Lawrence et al., 1994; Bigot et al., 1996; Papadimitriou et al., 1996; Heinrich et al., 1999). The relatively lower % ash (62–65%) in the young fawn (including fetal) bones is consistent with data demonstrating lower mineral content in neonate mammals compared to adults of the same species (Carrier, 1983; Currey and Pond, 1989; Brear et al., 1990; Heinrich et al., 1999). However, the % ash values in the young fawns of the present study are higher than some neonate mammals, consistent with data supporting the idea that limb bones of neonate precocial animals have relatively higher % ash (providing relatively greater stiffness) than do neonate altricial animals (e.g., 57–60% in femora of neonate precocial rabbits and muskoxen [Carrier, 1983; Heinrich et al., 1999] vs. about 50% ash in the femur of a 4-week-old altricial dog [Torzilli et al., 1981]). However, the mechanical/adaptive relevance of mineral content variations in the young fawn age group must be interpreted cautiously since some of these bones

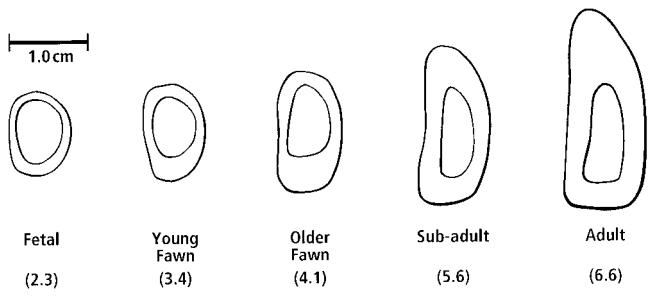

Fig. 6. Ontogenetic changes in cross-sectional geometry of the mule deer calcaneus at 60% diaphyseal length. Numbers in parentheses indicate bone "length" in cm.

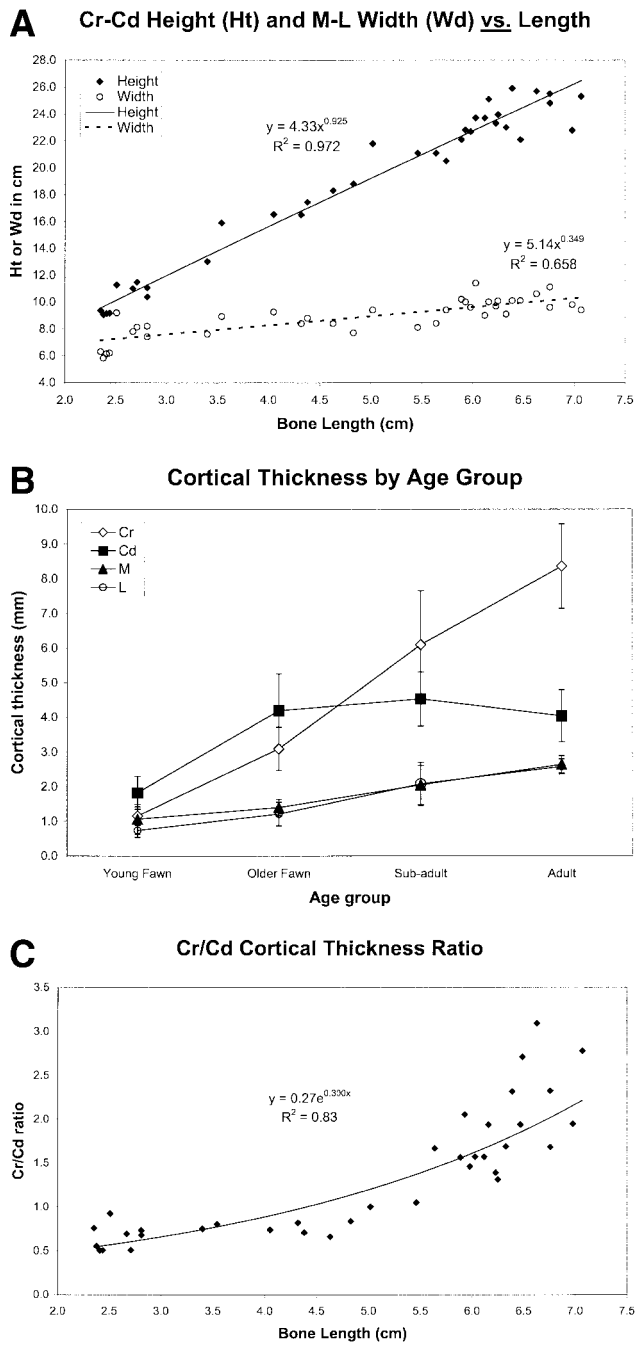

Fig. 7. Cortical Thickness. **A:** Linear plot of "height" and "width" vs. length. **B:** Average cortical thickness by age group. The cranial cortex increases in a near-linear fashion while each of the other cortices shows little increase in thickness after the older fawn age group. Note that the caudal cortex actually decreases from subadult to adult age groups. **C:** Cranial:caudal cortical thickness ratio vs. bone length. The ratio begins to increase at the subadult stage.

exhibited highly mineralized tissue that appears to be residual calcified cartilage.

General implications of regional material variations. The progressive regional changes in material organization (e.g., % ash, secondary osteon population density [N.On/Ar], predominant CFO) may represent responses to the tension/compression/shear strain distribution (Fig. 1). As noted, this would be expected since cortical bone is substantially stronger and stiffer, has different fatigue behavior, and likely has greater toughness in compression than in tension or shear. However, increasing both cortical

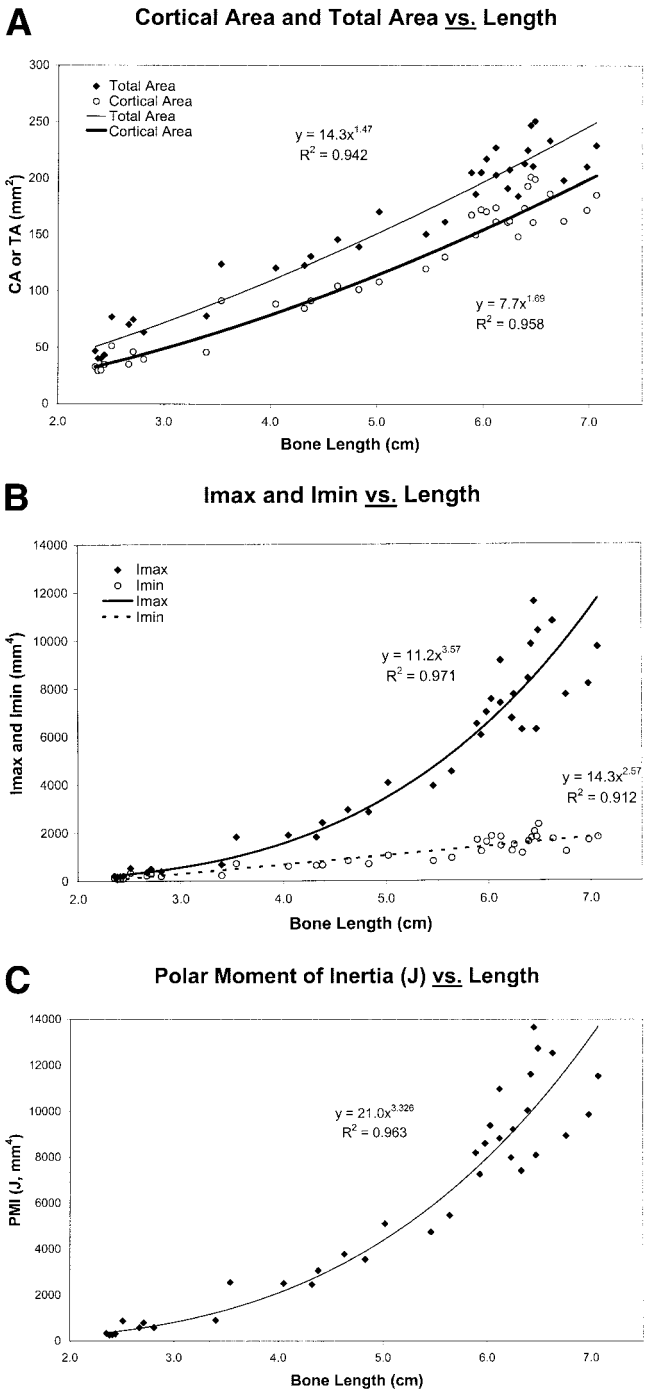

Fig. 8. Geometry. **A:** Cortical area and total area vs. bone length. **B:** Imax and Imin vs. bone length. **C:** Polar moment of inertia (J) vs. bone length.

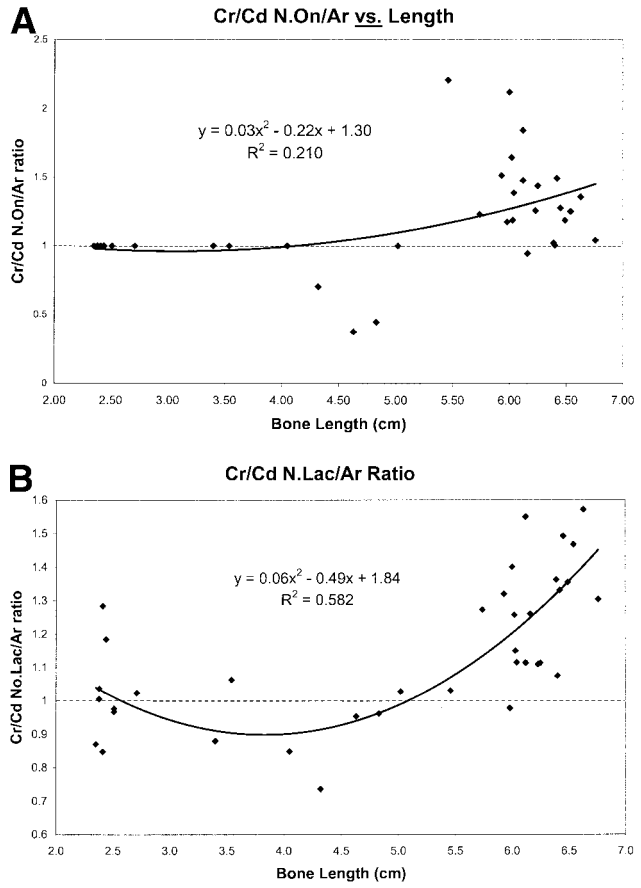

Fig. 9. N.On/Ar and N.Lac/Ar. **A:** Cranial:caudal ratio of secondary osteon population density (N.On/Ar) vs. bone length. **B:** Cranial:caudal ratio of osteocyte lacuna population density (N.Lac/Ar) vs. bone length.

thickness *and* mineral content in the relatively more yield-resistant compression region of the mule deer calcaneus seems redundant in the context of stiffness and strength. The material variations may therefore enhance other important mechanical properties in each loading mode, including energy absorption and fatigue resistance (Currey, 1969, 1984a,b; Martin and Burr, 1989; Reilly et al., 1997; Shelton et al., 2000; Skedros et al., 2000a, 2001c,d, 2002a, 2003a). Regional and ontogenetic increases in these properties can be achieved by adjusting predominant CFO, % ash, porosity, and osteonal remodeling (Martin et al., 1996; Zioupos and Currey, 1998; Yeni et al., 1997, 2001; Les et al., 2002; Skedros et al., 2000a, 2002a, 2003a–c). Similar to subadult and adult deer calcanei, secondary osteons in the habitual "compression" cortices of equine radii and sheep calcanei have also been shown to have predominantly oblique-to-transverse CFO compared to the opposing "tension" cortices (Riggs et al., 1993a; Mason et al., 1995; Skedros et al., 2002a). In equine radii and third metacarpals, nonuniform CFO patterns enhance energy absorption and impact strength (Riggs et al., 1993b; Batson et al., 2000; Skedros et al., 2000a, 2001c). Recent studies have also shown an important role for CFO in energy absorption in cranial and caudal cortices of deer calcanei when tested in their habitual loading mode (compression and tension, respectively) (Skedros et al., 2001d, 2003a).

Transition from primary bone to secondary bone. The relative abundance of primary bone in the calcaneus and other bones of the developing artiodactyl appendicular skeleton may reflect relatively faster growth rates that are required for precocial ambulation (compared to, for example, more secondary osteons in appendicular skeletons of altricial humans) (Enlow and Brown, 1958; Currey, 1960; Stover et al., 1992; Skedros et al., 2003c). Experimental data available through the 1980s suggested that primary bone is stronger and more fatigue resistant than more extensively remodeled (secondary osteon) bone (Wright and Hayes, 1976; Carter et al., 1976; Currey, 1975, 1984a). This was attributed to a "weakening" effect of secondary osteons, since they presumably reduce tissue and volumetric mineral content by reducing mean tissue age and increasing porosity, respectively, and create an inherently weaker structure by increasing cement line and lamellar interfaces. More recent studies,

*TABLE 7. Allometric relationships between bone length and geometric characteristics in the mule deer calcaneus**

		All ages included (n = 36)			Subadult and adult (n = 22)			Fawn groups only (n = 14)		
Regression	Isometry	RMA slope	95% CI	r	RMA slope	95% CI	r	RMA slope	95% CI	r
Bone length vs.										
Average height	1.0	0.937	0.88–0.99	0.986	0.796	0.56–1.03	0.785	1.039	0.88–1.19	0.972
Average width	1.0	0.431	0.35–0.52	0.811	0.931	0.57–1.29	0.583	0.633	0.34–0.92	0.672
Cortical area	2.0	1.671	1.55–1.79	0.979	1.981	1.48–2.48	0.819	1.824	1.41–2.23	0.934
Total area	2.0	1.496	1.37–1.62	0.971	1.649	1.17–2.12	0.762	1.818	1.38–2.26	0.928
Section modulus (Z)	3.0	2.629	2.45–2.81	0.979	3.016	2.23–3.80	0.813	2.948	2.34–3.55	0.945
Imax	4.0	3.597	3.37–3.82	0.984	3.803	2.81–4.80	0.811	4.012	3.30–4.73	0.962
Imin	4.0	2.656	2.37–2.94	0.955	3.369	2.25–4.49	0.697	3.319	2.33–4.31	0.887
PMI (J)	4.0	3.361	3.13–3.59	0.933	3.676	2.70–4.65	0.804	3.798	3.00–4.59	0.947

*RMA, reduced major axis regression; CI, confidence interval; r, correlation coefficient; PMI, polar moment of inertia.

however, have shown that primary bone is superior to remodeled bone in terms of minimizing microcrack formation, but *inferior to remodeled bone* in terms of attenuating the distance and rate of microcrack propagation (Yeni et al., 1997; Reilly et al., 1997; Reilly and Currey, 1999). Accommodating microdamage accumulation allows the absorption of a substantial amount of energy by increasing the compliance of the bone material and improving tolerance of larger deformations for a given load (Reilly and Currey, 1999). In this context, remodeled bone may enhance fatigue properties to a greater extent than primary bone. The progressive remodeling in the developing cervine calcaneus might similarly enhance fatigue resistance.

Progressive age-related remodeling also substantially influences bone vascularity. For example, in a study of the vascular network of an ontogenetic series of canine tibiae, Marotti and Zallone (1980) noted that as secondary osteons are formed and their canals narrow, there is a progressive reduction in the number of vessels in each canal. However, there is evidence that the maximum distance between osteocytes and vessels is less in primary bone than in secondary bone (Dempster and Enlow, 1959; Currey, 1960). Although it has been suggested that increased percentage of secondary bone results in increased porosity (and hence vascularity) (Schaffler and Burr, 1988; Burr et al., 1990), data in artiodactyl calcanei suggest an exception to this tenet (Skedros et al., 1997). Therefore, remodeling, although undoubtedly important for enhancing blood flow in some specific conditions, may not be primarily aimed at enhancing vascularity. As noted below, improving matrix quality may be more important in this regard. It is suggested that some features of vascular channel organization (e.g., orientation and concentration) that are established in the primary bone of the mule deer calcaneus are largely influenced by genetically derived positional information. In contrast, secondary osteons that subsequently form may be more strongly influenced by strain transduction and microdamage effects. However, to some degree, there may be a strong genetic component for some remodeling events. This is supported by limited studies showing that the locations of secondary osteons in paired limb bones have a quasi-symmetrical (i.e., mirror image) distribution in animals that do not show, or have minimal evidence of, limb dominance (Marotti, 1963; Currey, 1984a; Dempster, 1992; R.A. Walker, pers. commun.). However, studies that rigorously examine this issue are warranted since Burr (1993) has offered cogent arguments to the contrary.

Bone histology can also be influenced by growth rate, and this is most evident in primary bone. However, the quantitative studies that address this issue are few; the most rigorous have used avian long bones (de Margerie et al., 2002). In our microscopic images, the inferred spatial-temporal differences in appositional growth rates between the cranial and caudal cortices are most notable as circumferential lamellae along the periosteal margin of the cranial cortex.

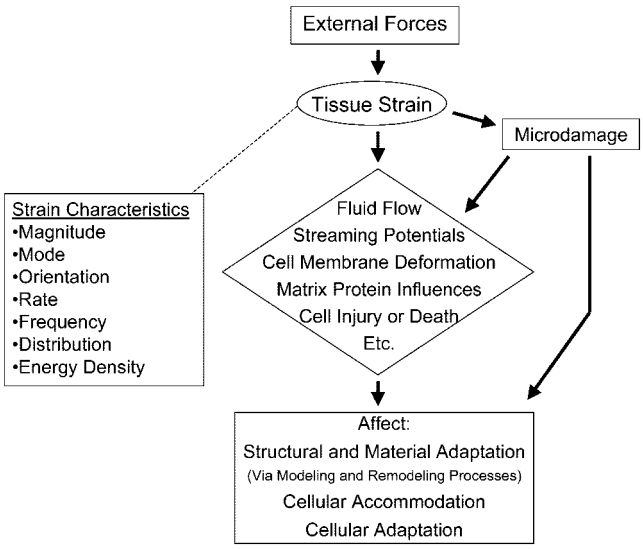

Fig. 10. Possible bone stimulus-response algorithm. Tissue strain may not be as proximate in influencing bone adaptation as are, for example, fluid-flow dynamics and other biomechanical or biochemical stimuli. In some cases, microdamage may be an important event in affecting adaptation during normal development. Cellular accommodation refers to the ability of bone cells to adjust to their physical and biochemical environment. This concept is discussed in detail by Turner (1999).

Role for microdamage in mediating regional material variations. Nonuniform CFO, N.On/Ar, and/or other remodeling-mediated variations might also serve to differentially "toughen" the cortex by minimizing regional disparities in microdamage accumulation and/or propagation in "tension," "compression," and "shear" regions (Skedros et al., 1995; Reilly et al., 1997; Boyce et al., 1998; Reilly and Currey, 1999). Regional disparities in microdamage incidence (i.e., formation frequency) and morphologic characteristics (e.g., microcrack length, shape, and orientation) (Taylor and Lee, 1998; Boyce et al., 1998) may represent the "mechanism" that drives the regional and age-related histologic differences shown in the present study, and between "tension" and "compression" cortices of other limb bones, including the mid-diaphyses of ovine and equine radii, sheep calcanei, and equine third metacarpals, and human proximal femoral diaphyses (Lanyon et al., 1979; Riggs et al., 1993a,b; Mason et al., 1995; Lee et al., 1999; Skedros et al., 1996a, 1999, 2002a) (Fig. 10).

Previous studies characterize fatigue of cortical bone as a steady and progressive reduction in modulus leading to ultimate failure (Carter and Hayes, 1976, 1977; Carter et al., 1981a,b). However, in vitro experiments by Schaffler et al. (1989, 1990) in cortical bone of bovine femora and tibiae showed that cyclic loading caused a gradual decrease in modulus

only during the first few million loading cycles. After the initial stiffness loss, specimen modulus stabilized and did not appear to change for the duration of the experiment. They noted that this behavior in bone resembles fatigue behavior in fiber-reinforced composites such as graphite and laminated plastic, where microdamage occurs *early in loading history* and the loss of material stiffness corresponds to increased numbers of cracks. In view of these data, it is plausible that there may be a regionally increased prevalence of microcracks early in a limb bone's development, and that such differences may be eliminated or minimized by subsequent repair-directed remodeling (Martin, 2002; Skedros et al., 2003c). Further studies in ontogenetic series of animals are needed to determine if microdamage events are important influences in the progressive regional microstructural and ultrastructural reorganization that occurs in the developing mule deer calcaneus.

Osteocyte lacuna population density: mechanical/metabolic implications. Since osteocyte lacunae may become locations where microdamage is more likely to occur (i.e., stress-risers) (especially with age or excessive exercise; Reilly, 2000) and osteocytes may be the "sensors" of microdamage (Martin, 2000; Vashishth et al., 2000), modifying their concentrations may be a means for enhancing a bone's fatigue life. The present study showed that N.Lac/Ar is significantly higher in the "compression" (cranial) cortex vs. the "tension" (caudal) cortex, and this difference increased with age. These results are consistent with past studies of adult artiodactyl and equine calcanei demonstrating significantly higher N.Lac/Ar in "compression" vs. "tension" cortices (horse: 650 ± 71 vs. 599 ± 110; elk: 732 ± 55 vs. 644 ± 62; sheep: 710 ± 65 vs. 609 ± 64; $P < 0.05$ for all comparisons) (Hunt and Skedros, 2001). However, equine third metacarpals demonstrate *lower* N.Lac/Ar in cortical locations habitually loaded in "compression" vs. "tension" (425 ± 77 vs. 533 ± 91, $P < 0.001$) (Skedros et al., 2000b). In contrast, equine radii showed *higher* N.Lac/Ar in "compression" vs. "tension" cortices (522 ± 128 vs. 478 ± 138, $P < 0.05$) (Skedros et al., 1996b). Although these differences in equine radii are statistically significant, this would increase the distance between any two osteocytes by ~2 μ, suggesting little functional advantage. Additionally, in these two equine bones N.Lac/Ar did not correlate with transcortical strain magnitudes (Skedros et al., 2000b; Hunt and Skedros, 2001). Recent mechanical testing data from adult mule deer calcaneal cortices also show that variations in N.Lac/Ar explain little, if any, variance in pre- and postyield mechanical properties, including energy absorption (Skedros et al., 2003b, and unpubl. data). Therefore, regional variations in N.Lac/Ar appear to be epiphenomena in a mechanical context—N.Lac/Ar may be correlated with other histocompositional parameters (such as N.On/Ar or % ash; see below) that are relatively more important in influencing mechanical properties. While local strain mode and magnitude may not be directly involved in differential recruitment of osteoblasts (Fig. 10), mechanisms of nutritional delivery (e.g., vascular transport, matrix convective fluid flow, diffusion, etc.) and metabolic requirements are probably the most important factors in limiting the density of these cells (Mullender and Huiskes, 1997; Knothe Tate et al., 1998; Fyhrie and Kimura, 1999).

Secondary osteon size, shape, and population density. Consistent with data in previous studies (Skedros et al., 1994a, 1997, 2001a), observations in the present study reveal that osteons in the highly strained cranial "compression" cortex of subadult and adult calcanei are smaller, more circular, and more numerous than osteons in the opposing, relatively less strained "tension" cortex. It has been hypothesized that osteon cross-sectional area can be reduced in states of increased loading (Abbott et al., 1996). There is indirect evidence that regional osteon cross-sectional size variations, such as those observed between the cranial and caudal cortices of the deer calcanei, can influence toughness (Yeni et al., 1997).

Recent mechanical testing studies have been conducted to specifically clarify the contributions of various histocompositional characteristics on cortical bone mechanical properties of deer calcanei in the physiologic context of "strain-mode-specific" testing (e.g., compression testing of the habitually compression-loaded cranial cortex; tension testing of the habitually tension-loaded caudal cortex) (Skedros et al., 2001d, 2003a,b). Multiple regression analyses show that in compression of the cranial ("compression") cortex, secondary osteon population density is the most important variable in explaining variance in energy absorption, and third or fourth most important variable in explaining elastic modulus, yield stress, and ultimate stress. Variances in these latter three variables are best explained by osteon cross-sectional shape, predominant CFO, and/or porosity. In contrast, predominant CFO and porosity are the first and second most important explanatory variables, respectively, in tension testing of the caudal ("tension") cortex. Osteon cross-sectional area was influential only in yield stress (the third most important explanatory variable) in tension testing of the caudal cortex.

In cranial vs. caudal comparisons, significantly smaller osteons occur in the highly strained cranial cortices of the calcanei of adult mule deer, but this difference is not statistically significant in subadult bones ($P = 0.32$) (Skedros et al., 2001a). Our observations suggest that this strain-magnitude-related association is not present in fawns. Significantly smaller osteons occur in the highly strained cranial ("compression") cortices of adult ovine (e.g., sheep)

and equine (e.g., horse) calcanei (Skedros et al., 1994b, 1997). However, this association is *not* present in other "tension/compression" bones, including mid-diaphyses of adult ovine and equine radii and equine third metacarpals (Mason et al., 1995; Skedros et al., 1996a; Skedros, 2001). Considerable variability in microstructural morphologies and remodeling dynamics can occur in different locations within a single bone (Marotti, 1976; Stout, 1984; Brand, 1992; Bell et al., 2001). Furthermore, variations in osteonal cross-sectional shape, area, and population densities are not considered reliable characteristics for interpreting tissue adaptations to the predominant strain distribution of a habitual bending history (Skedros et al., 1996a; Skedros, 2000, 2001). These considerations support the probability that there are a variety of mechanical and metabolic mechanisms driving the BMU remodeling events that produce osteon numbers and their cross-sectional areas and shapes (Heřt et al., 1972; Richman et al., 1979; Currey, 1984a; Burr, 1993; Bouvier and Hylander, 1996; Pfeiffer, 1998; Brown, 2000; Jordan et al., 2000; Bell et al., 2001). Thus, discretion must be exercised when formulating hypotheses about seemingly straightforward correlations between microstructure and specific mechanical features.

Formation of Nonuniform Predominant Collagen Fiber Orientation (CFO) Patterns: Evidence of Differential Influences of Variant vs. Invariant Strain Stimuli?

Riggs et al. (1993a) demonstrated that young equine (foal) radii at mid-diaphysis lack secondary osteons, and that an entire cross-section appears relatively homogeneous under circularly polarized light, suggesting no significant regional differences in predominant CFO. Secondary osteons, which subsequently form in the cranial ("tension") cortex produce/retain the more longitudinal collagen fibers, whereas secondary osteons that form in the caudal ("compression") cortex produce more oblique-to-transverse fibers. (Note that the *cranial* horse radius receives habitual *tension* in contrast to the *cranial* deer calcaneus, which receives habitual *compression*.) The CFO differences between the cranial and caudal cortices of subadult and adult deer calcanei are also correlated with secondary osteon formation. Predominant CFO, however, is not correlated with transcortical strain magnitude variations in the horse radius (Mason et al., 1995). These results suggest that cortical bone tissue is relatively sensitive to tension and compression strain *modes*, which are *variant* (i.e., vectorial) components of the strain milieu (in contrast to invariant components such as strain energy density and strain magnitude) (Rubin et al., 1990; Turner, 1991; Brand and Stanford, 1994; Skedros et al., 1996a, 1998, 2001b; Skedros, 1994, 2001; Goodwin and Sharkey, 2002). Additionally, as discussed below, prevalent shear stresses may be important influences in producing the relatively more oblique-to-transverse CFO observed in the medial and lateral cortices (compared to the cranial "compression" cortex) of subadult and adult deer calcanei.

Cellular mechanisms of "strain-mode-specific" CFO patterns. A recent study by Takano et al. (1999) supports a *causal* relationship between changes in prevailing strain mode distribution and topographic CFO patterns shown in the present study. Using diaphyses of adult canine radii, they demonstrated that experimentally induced alterations in a physiologic tension/compression strain distribution—which substantially moved the location of the neutral axis—caused changes in CFO and mineral growth. Specific strain modes and/or the microdamage that they produce may therefore be linked to stimuli that are more proximate and more critical to the attainment of adapted tissue morphology (e.g., strain gradients and related phenomena such as fluid flow and streaming potentials) (Fig. 10) (Judex et al., 1997a,b; Srinivasan and Gross, 2000; Judex and Zernicke, 2000; Smit et al., 2002). By inducing cellular mechanisms (e.g., gene expression), tension, compression, and shear strains may enable differential remodeling responses and/or produce regionally nonuniform collagenous or non-collagenous protein organization and/or expression (Yeh and Rodan, 1984; Skerry et al., 1990; Ingram et al., 1994; Rubin et al., 1996; Su et al., 1997; Terai et al., 1999; Ikegame et al., 2001).

Strain Magnitudes and Directions, and Other Mechanical and Nonmechanical Factors

In a study of functional strains on calcanei of adult mule deer, Su et al. (1999) showed that shear strains in the medial and lateral cortices, when compared to those in the cranial and caudal cortices, were aligned more closely to the long axis of the bone. In turn, principal strains in medial and lateral cortices deviated some 24–27° from the long axis. The possibility that principal strain directions influence the ultrastructural/microstructural features that distinguish the medial and lateral cortices from the cranial and caudal cortices is suggested by associations of osteon orientation and/or collagen anisotropy with principal strain direction (Lanyon and Bourn, 1979; Martin and Burr, 1989, pp. 158–159, 167–173; Heřt et al., 1994; Petrtýl et al., 1966; Takano et al., 1999). A postulated mechanism for this relationship is that osteoclast/osteoblast units detect and follow directions of maximum principal strain and/or strain/fluid-flow gradients during osteon formation (Martin and Burr, 1989, pp. 167–173; Robling and Stout, 1999; Smit and Burger, 2000; Smit et al., 2002). If this were correct, then the secondary osteons in medial and lateral cortices

should be obliquely oriented with respect to the long axis of the calcaneus. This is supported by qualitative observations in subadult and adult calcanei in the present study, and by quantitative data in calcanei of adult sheep, deer, elk, and horses (Skedros et al., 1994b, 1997) showing that secondary osteons typically have oblong cross-sectional shapes in transversely sectioned medial and lateral cortices compared to the comparatively more circular osteons of the cranial and caudal cortices. In addition, oblique osteon orientations may be the physical basis for the notably more oblique-to-transverse CFO in the medial and lateral cortices compared to the cranial and caudal cortices of the subadult and adult bones. One functional explanation for such tissue heterogeneity is that it reduces potentially deleterious local lamellar shear stresses within osteons and/or between osteons and the interstitial matrix (Martin and Burr, 1989, pp. 158–159; Norman and Wang, 1997; Brown et al., 2000; Yeni and Norman, 2000; Goodwin and Sharkey, 2002). Shear stresses can also be produced by any loading mode causing principal stresses at some angle to the diaphyseal axis (Drucker, 1967). Shear stresses produced in the cranial and caudal cortices, although of relatively lower magnitude, may also have some influence on the material differences between these regions.

Distinctive biomechanics and "peculiar" organization of the caudal cortex. Among all cortical regions examined in the deer calcanei, the biomechanics of the caudal cortex are distinctive because this region: 1) forms an attachment for the plantar ligament (Fig. 1), and 2) is significantly stress-shielded by the plantar ligament and the tendon of the superficial digital flexor muscle (Su et al., 1999). Local reductions in strain, or locally increased perfusion, etc., have been offered as possible explanations for the "peculiar" organization of the caudal cortex in subadult and adult animals; namely, the relatively increased porosity and remodeling activity (low % ash and high NREs), and large and irregularly shaped osteons (Skedros et al., 1994b, 1997; Su et al., 1999). Even if this interpretation is correct, the presence of collagen fibers with preferred longitudinal orientation in the caudal cortex suggests an important role for strain mode (Skedros et al., 2000c; Skedros, 2001), which is a specific strain feature that is not typically considered an important stimulus in bone material construction (Skedros et al., 2001a). The thickness of the caudal cortex also increases at a faster rate than the cranial cortex during earlier phases of growth (Figs. 6, 7). This may represent programmed development that rapidly matures this attachment site with minimal strength reduction resulting from prolonged modeling activity (Enlow, 1962; Hoyte and Enlow, 1966).

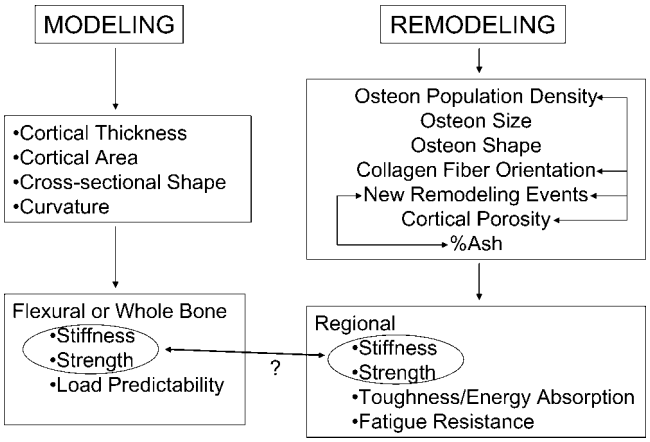

Fig. 11. Modeling and remodeling: "A division of labor." Development of the mule deer calcaneus is produced by both modeling processes, affecting whole-bone stiffness and strength, and regional remodeling processes, influencing local material properties. A structural vs. material "division of labor" between modeling vs. remodeling, respectively, appears to exist in the developing mule deer calcaneus. Interrelationships among the material characteristics are shown with arrows. Question mark (?) indicates that it is controversial whether or not regional stiffness and strength in a bone diaphysis are strongly influenced by remodeling-mediated characteristics.

Mechanical Relevance of Structural Variations

Modeling vs. remodeling: loading predictability and division of labor. It has been proposed that *structural* variations within an appendicular long bone are most strongly selected for enhancing "loading predictability" during typical use (Rubin, 1984; Lanyon, 1987; Bertram and Biewener, 1988; Swartz, 1990; Les, 1995; Skedros et al., 1996a). This, in turn, reduces the risk for fracture while ensuring the presence of important strain-related signals for limb-bone tissue/organ growth and maintenance (Lanyon, 1980, 1987; Currey, 1984a, 1988a,b; Bertram and Biewener, 1988; Skedros et al., 1996a, 2003c). Loading predictability therefore appears to be a major goal of a bone's naturally selected adapted morphology (Fig. 11). In the cervine tarsus, loading predictability is primarily ensured by articular morphology, which confines talocalcaneal motion to the sagittal plane (Alexander and Bennett, 1987). Analytical studies in other bones with more variable bending (e.g., equine principal metacarpals) also suggest that remodeling-related material variations such as secondary osteon population density, predominant CFO, and % ash have little or no influence on loading predictability (Gross et al., 1992; Les, 1995, and pers. commun.). This is because a predictable, and hence controlled, strain environment is readily achieved and accommodated by *modeling* processes, which produce variations in *structural* characteristics including bone cortical thickness and cross-sectional shape, which in turn affect whole-bone

stiffness and strength (Bertram and Biewener, 1988; Les, 1995; Skedros et al., 1996a, 2003d). In contrast, the regional *remodeling* activities produce the material heterogeneities that result in important influences on local *material* properties. Consequently, a structural vs. material "division of labor" mediated by modeling vs. remodeling activities, respectively, appears to be at work in the developing mule deer calcaneus.

Dimensional scaling relationships. Analysis of scaling relationships showed that structural asymmetry of the calcaneus is established relatively early, rapidly satisfying the mechanical requirements of a short, rigid in-lever. Negative allometries are prevalent (Table 7) and are most evident along the medial–lateral axis (direction of Imin). The resulting cranial–caudal elongation reflects the formation of a rectangular or quasi-I-beam cross-section, enhancing the cross-sectional moment of inertia in the direction of preferential bending (Wainwright et al., 1982). In subadults and adults, only the cranial cortex showed a significant increase in cortical thickness. Thus, the appearance of relatively greater negative allometries along the cranial–caudal axis would be expected in older bones.

Carrier and Leon (1990) showed negative allometry of mid-diaphyseal diameter in the hindlimb long bones of California gulls. They argue that this negative allometry permits the rapidly growing hindlimb to function in locomotion shortly after hatching. Heinrich and co-workers showed that bone length scales with negative allometry on body mass in mustelid humeri and femora (Heinrich and Biknevicius, 1998) and muskoxen femora (Heinrich et al., 1999). In the muskoxen femora this effect was attributed to neonate animals. In contrast, these investigators showed that bone robusticity (cross-sectional parameters against bone length) scales with strong positive allometry in these mustelid bones. Previous analyses of skeletal allometry of various large terrestrial Carnivora and Bovidae also show that in impact-loaded long bones, bone length and cross-sectional geometric parameters (e.g., mid-diaphyseal diameter) scale with positive allometry (Bertram and Biewener, 1990). However, as discussed below, relationships of bone cross-sectional robusticity and functional usage that help explain these relationships in the limb long bones of these various species do not appear to be at work in the developing deer calcaneus.

Clearly, ontogenetic skeletal scaling relationships are complex because a bone's material and geometric properties can change at different rates during development (Sumner, 1984; Heinrich et al., 1999; Carrier and Leon, 1990), and this is especially evident in the deer calcaneus. However, comparing scaling relationships shown in the present study with those reported in *long bones* of other species must be made cautiously since: 1) relationships between length and cross-sectional geometric properties are more appropriate in long bones, where principles of beam theory are more applicable (Ruff, 1983, 1989), and 2) by being a short in-lever that is not aligned with the vector of weight-bearing impact, the deer calcaneus has different mechanical requirements compared to nearby long bones, which receive impact loads (Gambaryan, 1974; Hildebrand and Goslow, 2001). Additionally, even in long bones, it has been suggested that the mechanical factors affecting length and diameter are not the same, and therefore there may not be a consistent scaling relationship between these parameters among different species (Sumner, 1984; Bertram and Biewener, 1990; Christiansen, 1999). This seems even more relevant when comparing length and cross-sectional geometric properties of the short, tapered, in-lever construction of the deer calcaneus—where lever mechanics are satisfied primarily by bone length, and bending rigidity primarily by cross-sectional shape and robusticity.

The absence of isometric scaling or positive allometry along the cranial–caudal axis in subadult and adult deer calcanei may also be influenced by important load-carrying tissues that are not considered in the analysis of cross-sectional geometric properties. Such tissues include cancellous bone, which fills the medullary canal along 50–60% of the diaphysis, and the load-sharing function of the plantar ligament and superficial digital flexor tendon (Su et al., 1999). Additionally, heterogeneous cortical organization (e.g., relatively high mineral content in the cranial cortex) may enhance bending rigidity along the cranial–caudal axis.

Genetic, Epigenetic, and Extragenetic Influences in Developmental Adaptation

Intrauterine motion/loads: when does strain history begin to modify morphology? Contrary to our expected findings, the fetal bones in the present study showed arched trabecular patterns, a quasi-elliptical cross-sectional shape, and asymmetric cortical thickness in the plane of bending. Do these findings reflect genetically programmed development, or are they extragenetic (i.e., environmentally induced) products of strain history? It is possible that some of these characteristics may be controlled and constrained by intrinsic genetic and epigenetic factors that are largely independent of mechanical stimuli. For example, the systematic expression of genetically derived positional information (Raff, 1996; Wolpert, 1981, 1996; Wolpert et al., 1998) may be more directly important to a bone's development than any individual effects of strain transduction (Carter and Wong, 1988; Rubin et al., 1992; Lovejoy et al., 1999, 2002; Skedros and Brady, 2001; Skedros et al., 2002b). In this context, Lovejoy et al. (2002, pg. 100) state that:

> mounting evidence suggests that the role of mechanotransduction, especially in the developing/growing skel-

> eton, is to provide necessary *threshold* values required for implementation or maintenance of patterns of growth guided principally by positional information, and it seems increasingly likely that this maxim holds as much for cancellous bone (i.e., trabecular distribution and orientation) as it does for cortex.

Even bone density (g/cc) is now thought to be "…under strong genetic regulation" (Beamer et al., 1996, p. 397). Consequently, the simple assumption that the forces a bone experiences are primary, or even secondary in guiding its morphological formation is currently in question (Biewener and Bertram, 1993; Lovejoy et al., 1999, 2002).

Consistent with these hypotheses, finite element analyses of Carter and colleagues (Carter and Wong, 1988; Carter and Beaupré, 2001) suggest that positional information has a dominant influence in the early stages of skeletal ontogeny. However, these investigators propose that positional information becomes less important once the basic bone anlagen is established; subsequently, a bone's development may be more strongly influenced by the impact of stress history on gene expression. Such studies, however, may be insufficient to substantiate this conclusion since finite element analyses merely demonstrate that "shifts" in developmental morphology can be crudely modeled by sophisticated computer techniques and procedures. In contrast, a growing body of data supports the possibility that pattern formation continues to dominate in this context and that the proposed "shift" from pattern formation to strain history may not occur (Lovejoy et al., 2003).

Experimental and observational studies suggest that the epigenetic influences of muscular loading in utero or in ovo can produce trabecular and cortical morphologies such as those described in the developing deer calcaneus (Carter and Wong, 1988; Carter et al., 1996). For example, Skerry (2000) describes the unpublished qualitative observation of Lanyon and Goodship, who, after transecting the Achilles tendon of a living fetal lamb, noted that subsequent prenatal growth produced disorganized trabeculae in the experimental calcaneus compared to the contralateral control. Although this isolated observation warrants verification, it may suggest an important role for prenatal loading. Other studies of stillborn full-term humans with congenital neuromuscular diseases have shown the presence of significant cortical thinning and prevalent fractures, their severity being correlated to the duration and degree of intrauterine akinesia (Rodríguez et al., 1988a,b). A study of curare-paralyzed rat fetuses showed similar findings (Rodríguez et al., 1992). Lanyon (1980) showed that depriving the rat tibia of normal mechanical function during its growth period (by unilateral sciatic neurectomy) resulted in a failure of this bone to attain its normal weight, thickness, cross-sectional shape, and longitudinal curvature. However, categorizing the results of these studies under the rubric "prenatal loading" may be precarious, since these aggressive perturbations likely introduce profound, and difficult to control for, insults to the delicate environment of cell-to-cell interactions/communication and fluid-flow dynamics during early growth.

The current literature is therefore unclear about the relative influences of genetic and epigenetic developmental bias and constraint vs. extragenetic (environmental) factors (e.g., strain transduction and microdamage events) on bone modeling and remodeling activities. The artiodactyl calcaneus appears to be a good model for further examination of these issues because of its nonuniform structural and material organization, spatial/temporal variations in the emergence of specific characteristics of this organization (e.g., trabecular anisotropy early in development, and significant cranial:caudal CFO differences later in development), and simple loading regime that presumably persists throughout ontogeny.

CONCLUSIONS

From developmental geometric scaling relationships to regional variations in predominant collagen fiber orientation (CFO), the modifications that occur in the mule deer calcaneus appear to be strongly influenced by its habitual tension/compression strain distribution. In turn, many levels of its hierarchical organization may be aimed at satisfying its role as a short cantilever in a simple bending environment. Determining the influence of strain-related stimuli on the heterogeneous morphology of this bone represents a fruitful avenue for further research, since these mechanisms are probably also at work in the functional development of other appendicular bones.

Many of the structural variations that occur during early development of the mule deer calcaneus (e.g., arched trabeculae) may be strongly influenced by genetic- or epigenetic-derived processes. In contrast, some of the material variations that appear later (e.g., secondary osteon population density [N.On/Ar] and predominant CFO) may be products of extragenetic factors, including strain transduction and microdamage events. For example, similarities between regional differences in predominant CFO in the habitual "tension" and "compression" cortices of subadult and adult deer calcanei and other "tension/compression" bones suggest that the recognition of strain modes or their byproducts are important factors in the development of these regional heterogeneities. These and other *material* variations may ultimately enhance mechanical properties, including energy absorption and fatigue resistance for each region's habitual strain mode. In contrast, in many cases other material characteristics may be epiphenomena in a mechanical context (e.g., osteocyte lacuna population densities [N.Lac/

Ar], and osteon cross-sectional shape or area), but may be correlated with other characteristics that may be more important in influencing mechanical properties (e.g., N.On/Ar, CFO, and % ash).

Recent mechanical testing studies have helped to clarify the functional advantages of regional heterogeneities or asymmetries of some structural and material characteristics of the artiodactyl calcaneus, but the mechanism(s) that produce them are not well defined. Rigorous studies aimed at examining relationships between specific proximate stimuli (e.g., fluid-flow dynamics) and ultimate stimuli (e.g., strain modes, strain magnitudes, strain energy densities, and microdamage events) produced by time-varying physiologic bone loading are needed to more critically evaluate the relative roles that these stimuli may have in mediating the spatial/temporal control of modeling and remodeling activities.

ACKNOWLEDGMENTS

The authors thank Mary Hunsaker, Pat Hunsaker, Demetrios Skedros, Angel Skedros, George Pappas, Andy "Boom Shot" Bloebaum, Doug George, Dale George, Karen George, Brett Wheelock, Jorge Daskalakis, and the State of Utah Division of Wildlife Resources for their assistance in collecting the bones used in this study. We thank Karl Jepsen for providing the SLICE algorithm adapted for NIH Image. We thank Kerry Matz for the illustrations and Gwenevere Shaw for clerical support. We thank Kent Bachus, Cameron Bevan, Barr Peterson, Dana Gingell, Betty Rostro, Sharon Stefanou Chirban, Shila Gambarpour, Christine Knapp Phillips, Mark Gunst, Gregory J. Skedros, and Milena Zirovich for technical support, Robert A. Walker for contributing his observations, Mark T. Nielsen and Christian Sybrowsky for reviewing the manuscript, and Dennis Bramble for originally suggesting to us to investigate the artiodactyl calcaneus as a model for bone adaptation.

LITERATURE CITED

Abbott S, Trinkaus E, Burr DB. 1996. Dynamic bone remodeling in later Pleistocene fossil hominids. Am J Phys Anthropol 99: 585–601.

Alberts B. 1994. Molecular biology of the cell, 3rd ed. New York: Garland.

Alexander R McN. 1998. Symmorphosis and safety factors. In: Weibel ER, Taylor CR, Bolis L, editors. Principles of animal design: the optimization and symmorphosis debate. Cambridge, UK: Cambridge University Press. p 28–35.

Alexander R McN, Bennett MB. 1987. Some principles of ligament function, with examples from the tarsal joints of the sheep (*Ovis aries*). J Zool (Lond) 211:487–504.

Anderson AE. 1981. Morphologic and physiological characteristics. In: Walmo OC, editor. Mule and black-tailed deer of North America. Lincoln: University of Nebraska Press. p 27–97.

Batson EL, Reilly GC, Currey JD, Balderson DS. 2000. Postexercise and positional variation in mechanical properties of the radius in young horses. Equine Vet J 32:95–100.

Beamer WG, Donahue LR, Rosen CJ, Baylink DJ. 1996. Genetic variability in adult bone density among inbred strains of mice. Bone 18:397–403.

Bell KL, Loveridge N, Reeve J, Thomas CDL, Feik SA, Clement JG. 2001. Super-osteons (remodeling clusters) in the cortex of the femoral shaft: influence of age and gender. Anat Rec 264: 378–386.

Bertram JEA, Biewener AA. 1988. Bone curvature: sacrificing strength for load predictability? J Theor Biol 131:75–92.

Bertram JEA, Biewener AA. 1990. Differential scaling of the long bones in the terrestrial carnivora and other mammals. J Morphol 204:157–169.

Bertram JEA, Swartz SM. 1991. The 'law of bone transformation': a case of crying Wolff? Biol Rev 66:245–273.

Biewener AA, Bertram JEA. 1993. Mechanical loading and bone growth in vivo. In: Hall BK, editor. Bone, vol. 7. Bone growth — B. Boca Raton, FL: CRC Press. p 1–36.

Biewener AA, Bertram JEA. 1994. Structural response of growing bone to exercise and disuse. J Appl Physiol 76:946–955.

Biewener AA, Thomason J, Goodship A, Lanyon LE. 1983a. Bone stress in the horse forelimb during locomotion at different gaits: a comparison of two experimental methods. J Biomech 16:565–576.

Biewener AA, Thomason J, Lanyon LE. 1983b. Mechanics of locomotion and jumping in the forelimb of the horse (*Equus*): in vivo stress developed in the radius and metacarpus. J Zool (Lond) 201:67–82.

Biewener AA, Swartz SM, Bertram JEA. 1986. Bone modeling during growth: dynamic strain equilibrium in the chick tibiotarsus. Calcif Tissue Int 39:390–395.

Biewener AA, Fazzalari NL, Konieczynski DD, Baudinette RV. 1996. Adaptive changes in trabecular architecture in relation to functional strain patterns and disuse. Bone 19:1–8.

Bigot G, Bouzidi AA, Rumelhart C, Martin-Rosset W. 1996. Evolution during growth of the mechanical properties of the cortical bone in equine cannon-bones. Med Eng Phys 18:79–87.

Bouvier M, Hylander WL. 1996. The mechanical or metabolic function of secondary osteonal bone in the monkey *Macaca fascicularis*. Archs Oral Biol 41:941–950.

Boyce TM, Fyhrie DP, Glotkowski MC, Radin EL, Schaffler MB. 1998. Microdamage type and strain mode associations in human compact bone bending fatigue. J Orthop Res 16:322–329.

Boyde A, Riggs CM. 1990. The quantitative study of the orientation of collagen in compact bone slices. Bone 11:35–39.

Brand RA. 1992. Autonomous informational stability in connective tissues. Med Hypotheses 37:107–114.

Brand RA, Stanford CM. 1994. How connective tissues temporally process mechanical stimuli. Med Hypotheses 42:99–104.

Brear K, Currey JD, Pond CM. 1990. Ontogenetic changes in the mechanical properties of the femur of the polar bear *Ursus maritimus*. J Zool (Lond) 222:49–58.

Bromage TG. 1992. Microstructural organization and biomechanics of Macaque circumorbital region. In: Smith P, Tchernov E, editors. Structure, function and evolution of teeth. London: Freund. p 257–272.

Brown MD. 2000. Patterns of osteon size, comparing Holocene hunter-gatherers and recent humans. Am J Phys Anthropol 30(Suppl):113.

Brown CU, Yeni YN, Norman TL. 2000. Fracture toughness is dependent on bone location — a study of the femoral neck, femoral shaft, and the tibial shaft. J Biomed Mater Res 49:380–389.

Burr DB. 1992. Orthopedic principles of skeletal growth, modeling and remodeling. In: Carlson DS, Goldstein SA, editors. Bone biodynamics in orthodontic and orthopedic Treatment. Ann Arbor: University of Michigan. p 15–50.

Burr DB. 1993. Remodeling and the repair of fatigue damage. Calcif Tissue Int 53(Suppl 1):75–81.

Burr DB, Ruff CB, Thompson DD. 1990. Patterns of skeletal histologic change through time: comparison of an archaic native American population with modern populations. Anat Rec 226: 307–313.

Burr DB, Turner CH, Naick P, Forwood MR, Ambrosius W, Hasan MS, Pidaparti R. 1998. Does microdamage accumulation affect the mechanical properties of bone? J Biomech 31:337–345.
Burstein AH, Currey JD, Frankel PVH, Reilly DT. 1972. The ultimate properties of bone tissue: effects of yielding. J Biomech 5:35–44.
Burstein AH, Reilly DT, Martens M. 1976. Aging of bone tissue: mechanical properties. J Bone Joint Surg 58-A:82–86.
Carrier DR. 1983. Postnatal ontogeny of the musculo-skeletal system in the black-tailed jack rabbit (*Lepus californicus*). J Zool (Lond) 201:27–55.
Carrier DR, Leon LR. 1990. Skeletal growth and function in the California gull (*Larus californicus*). J Zool (Lond) 222:375–389.
Carter DR. 1984. Mechanical loading histories and cortical bone remodeling. Calcif Tissue Int 36:S19–S24.
Carter DR. 1987. Mechanical loading history and skeletal biology. J Biomech 20:1095–1109.
Carter DR, Hayes WC. 1976. Fatigue life of compact bone. I. Effects of stress amplitude, temperature and density. J Biomech 9:27–34.
Carter DR, Hayes WC. 1977. Compact bone fatigue damage: a microscopic examination. Clin Orthop 127:265–274.
Carter DR, Wong M. 1988. Mechanical stresses and endochondral ossification in the chondroepiphysis. J Orthop Res 6:148–154.
Carter DR, Hayes WC, Schurman DJ. 1976. Fatigue life of compact bone. II. Effects of microstructure and density. J Biomech 9:211–218.
Carter DR, Smith DJ, Spengler DM, Daly CH, Frankel VH. 1980. Measurement and analysis of in vivo bone strains on the canine radius and ulna. J Biomech 13:27–38.
Carter DR, Caler WE, Spengler DM, Frankel VH. 1981a. Fatigue behavior of adult cortical bone: the influence of mean strain and strain range. Acta Orthop Scand 52:481–490.
Carter DR, Caler WE, Harris WH. 1981b. Resultant loads and elastic modulus calibration of long bone cross sections. J Biomech 14:739–745.
Carter DR, van der Meulen MCH, Beaupré GS. 1996. Mechanical factors in bone growth and development. Bone 18(Suppl):5S–10S.
Christiansen P. 1999. Scaling of the limb long bones to body mass in terrestrial mammals. J Morphol 239:167–190.
Currey JD. 1960. Differences in the blood-supply of bone of different histologic types. J Microscop Sci 101:351–370.
Currey JD. 1969. The mechanical consequences of variation in the mineral content of bone. J Biomech 2:1–11.
Currey JD. 1975. The effects of strain rate, reconstruction and mineral content on some mechanical properties of bovine bone. J Biomech 8:81–86.
Currey JD. 1984a. The mechanical adaptations of bones. Princeton, NJ: Princeton University Press.
Currey JD. 1984b. Effects of differences in mineralization on the mechanical properties of bone. Philos Trans R Soc Lond B Biol Sci 304:509–518.
Currey JD. 1988a. Strain rate and mineral content in fracture models of bone. J Orthop Res 6:32–38.
Currey JD. 1988b. Can strains give adequate information for adaptive bone remodeling? Calcif Tissue Int 36:118–122.
Currey JD, Butler G. 1975. The mechanical properties of bone tissue in children. J Bone Joint Surg 57:810–814.
Currey JD, Pond CM. 1989. Mechanical properties of very young bone in the axis deer (*Axis axis*) and humans. J Zool (Lond) 218:59–67.
de Margerie E, Cubo J, Castanet J. 2002. Bone typology and growth rate: Testing and quantifying 'Amprino's rule' in the mallard (*Anas platyrhynchos*). C.R. Biologies 325:221–230 Laminar bone as an adaptation to torsional loads in flapping flight. J Anat 201:521–526.
Dempster DW. 1992. Bone remodelling. In: Coe FL, Favus MJ, editors. Disorders of bone and mineral metabolism. New York: Raven Press. p 355–380.
Dempster WT, Enlow DH. 1959. Patterns of vascular channels in the cortex of the human mandible. Anat Rec 135:189–205.
Drucker DC. 1967. Introduction to mechanics of deformable solids. New York: McGraw Hill.
Emmanual J, Hornbeck C, Bloebaum RD. 1987. A polymethyl methacrylate method for large specimens of mineralized bone with implants. Stain Tech 62:401–410.
Enlow DH. 1962. A study of the post-natal growth and remodeling of bone. Am J Anat 110:79–101.
Enlow DH, Brown SO. 1958. A comparative histological study of fossil and recent bone tissues. III. Mammalian bone tissues. General discussion. Tex J Sci 10:187–230.
Fritton SP, Rubin CT. 2001. In vivo measurement of bone deformations using strain gauges. In: Cowin SC editor. Bone mechanics handbook, 2nd ed. Boca Raton, FL: CRC Press. p 8-1–8-41.
Frost HM. 1986. Intermediary organization of the skeleton, vols. I and II. Chapters 7 and 9. Boca Raton, FL: CRC Press.
Fyhrie DP, Kimura JH. 1999. NACOB presentation keynote lecture. Cancellous bone biomechanics. North American Congress on biomechanics. J Biomech 32:1139–1148.
Gambaryan PP. 1974. Adaptation to running in the Ungulata. In: How mammals run. New York: John Wiley & Sons. p 92–162.
Goodwin KJ, Sharkey NA. 2002. Material properties of interstitial lamellae reflect local strain environments. J Orthop Res 20:600–606.
Goss RJ. 1983. Deer antlers. Regeneration, function, and evolution. New York: Academic Press.
Gross TS, McLeod KJ, Rubin CT. 1992. Characterizing bone strain distributions in vivo using three triple rosette strain gauges. J Biomech 25:1081–1087.
Grynpas M. 1993. Age and disease-related changes in the mineral of bone. Calcif Tissue Int 53(Suppl 1):S57–S64.
Gunasekaran B, Constantz BR, Monjazeb M, Skedros J, Bloebaum RD. 1991. An effective way of assessing crosslinks of collagenous proteins in biomaterials and tissues. Transactions of the 17th Annual Meeting of the Society of Biomaterials, Scottsdale, AZ, vol. XIV:139.
Heinrich RE, Biknevicius AR. 1998. Skeletal allometry and interlimb scaling patterns in mustelid carnivorans. J Morphol 235:121–134.
Heinrich RE, Ruff CB, Adamczewski JZ. 1999. Ontogenetic changes in mineralization and bone geometry in the femur of muskoxen (*Ovibos moschatus*). J Zool (Lond) 247:215–223.
Heřt J, Pribylova E, Liskova M. 1972. Reaction of bone to mechanical stimuli. 3. Microstructure of compact bone of rabbit tibia after intermittent loading. Acta Anat 82:218–230.
Heřt J, Fiala P, Petrtýl M. 1994. Osteon orientation of the diaphysis of the long bones in man. Bone 15:269–277.
Hildebrand M, Goslow G. 2001. Analysis of vertebrate structure, 5th ed. New York: John Wiley & Sons.
Hinkle DE, Wiersma W, Jurs WG. 1979. Applied statistics for the behavioral sciences. Chicago: Rand McNally College. p 84–85.
Hoyte DA, Enlow DH. 1966. Wolff's law and the problem of muscle attachment on resorptive surfaces of bone. Am J Phys Anthropol 24:205–213.
Huja SS, Katona TR, Burr DB, Garetto LP, Roberts WE. 1999. Microdamage adjacent to endosseous implants. Bone 25:217–222.
Hunt KJ, Skedros JG. 2001. The role of osteocyte lacunae populations in interpreting loading history of bone. Am J Phys Anthropol 32(Suppl):83.
Ikegame M, Ishibashi O, Yoshizawa T, Shimomura J, Komori T, Ozawa H, Kawashima H. 2001. Tensile stress induces bone morphogenetic protein 4 in preosteoblastic and fibroblastic cells, which later differentiate into osteoblasts leading to osteogenesis in the mouse calvariae in organ culture. J Bone Miner Res 16:24–32.
Indrekvam K, Husby OS, Gjerdet NR, Engesaeter LB, Langeland N. 1991. Age-dependent mechanical properties of rat femur. Measured in vivo and in vitro. Acta Orthop Scand 62:248–252.
Ingram RT, Park YK, Clarke BL, Fitzpatrick LA. 1994. Age- and gender-related changes in the distribution of osteocalcin in the extracellular matrix of normal male and female bone. Possible

involvement of osteocalcin in bone remodeling. J Clin Invest 93:989–97.
Jee WSS, Li XJ, Ke HZ. 1991. The skeletal adaptation to mechanical usage in the rat. Cells Mater (Suppl 1):131–142.
Jepsen KJ, Davy DT. 1997. Comparison of damage accumulation measures in human cortical bone. J Biomech 30:891–894.
Jepsen KJ, Bensusan J, Davy DT. 2001. Inter-modal effects of damage on mechanical properties of human cortical bone. Trans Orthop Res Soc 26:13.
Jordan GR, Loveridge N, Bell KL, Power J, Rushton N, Reeve J. 2000. Spatial clustering of remodelling osteons in the femoral neck cortex: a cause of weakness in hip fracture? Bone 26:305–313.
Judex S, Zernicke RF. 2000. Does the mechanical milieu associated with high-speed running lead to adaptive changes in diaphyseal growing bone? Bone 26:153–159.
Judex S, Gross TS, Bray RC, Zernicke RF. 1997a. Adaptation of bone to physiological stimuli. J Biomech 30:421–429.
Judex S, Gross TS, Zernicke RF. 1997b. Strain gradients correlate with sites of exercise-induced bone-forming surfaces in the adult skeleton. J Bone Miner Res 12:1737–1745.
Kachigan SK. 1986. Statistical analysis: an interdisciplinary introduction to univariate & multivariate methods. New York: Radius Press.
Kalmey JK, Lovejoy CO. 2002. Collagen fiber orientation in the femoral necks of apes and humans: do their histological structures reflect differences in locomotor loading. Bone 31:327–332.
Keller TS, Lovin JD, Spengler DM, Carter DR. 1985. Fatigue of immature baboon cortical bone. J Biomech 18:297–304.
Knothe Tate ML, Knothe U, Niederer P. 1998. Experimental elucidation of mechanical load-induced fluid flow and its potential role in bone metabolism and functional adaptation. Am J Med Sci 316:189–195.
Lanyon LE. 1974. Experimental support for the trajectorial theory of bone structure. J Bone Joint Surg 56-B:160–166.
Lanyon LE. 1980. The influence of function on the development of bone curvature. An experimental study on the rat tibia. J Zool (Lond) 192:457–466.
Lanyon LE. 1987. Functional strain in bone tissue as an objective, and controlling stimulus for adaptive bone remodelling. J Biomech 20:1083–1093.
Lanyon LD, Baggott DG. 1976. Mechanical function as an influence on the structure and form of bone. J Bone Joint Surg 58-B:436–443.
Lanyon LE, Bourn S. 1979. The influence of mechanical function on the development and remodeling of the tibia: an experimental study in sheep. J Bone Joint Surg 61-A:263–273.
Lanyon LE, Magee PT, Baggott DG. 1979. The relationship of functional stress and strain to the processes of bone remodeling: an experimental study on the sheep radius. J Biomech 12:593–600.
Lawrence LA, Ott EA, Miller GJ, Poulos PW, Piotrowski G, Asquith RL. 1994. The mechanical properties of equine third metacarpals as affected by age. J Anim Sci 72:2617–2623.
Lee TC, Noelke L, McMahon GT, Mulville JP, Taylor D. 1999. Functional adaptation in bone. In: Pedersen P, Bendsoe M, editors. IUTAM symposium on synthesis in bio solid mechanics. Dordrecht: Kluwer. p 1–10.
Les CM. 1995. Material heterogeneity in the equine metacarpus: Documentation and biomechanical consequences. Ph.D. Dissertation. Davis: University of California.
Les CM, Stover SM, Keyak JH, Taylor KT, Kaneps AJ. 2002. Stiff and strong compressive properties are associated with brittle post-yield behavior in equine compact bone material. J Orthop Res 20:607–614.
Levenston ME. 1994. Simulation of functional adaptation in trabecular and cortical bone. Ph.D. Dissertation. Palo Alto, CA: Stanford University.
Levenston ME, Beaupré GS, Jacobs CR, Carter DR. 1994. The role of loading memory in bone adaptation simulations. Bone 15:177–186.
Lewall EF, Cowan IM. 1963. Age determination in black-tailed deer by degree of ossification of the epiphyseal plate in the long bones. Can J Zool 41:629–636.
Lovejoy CO, Cohn MJ, White TD. 1999. Morphological analysis of the mammalian postcranium: A developmental perspective. Proc Natl Acad Sci USA 96:13247–13252.
Lovejoy CO, Meindl RS, Ohman JC, Heiple KG, White TD. 2002. The Maka femur and its bearing on the antiquity of human walking: applying contemporary concepts of morphogenesis to the human fossil record. Am J Phys Anthropol 119:97–133.
Lovejoy CO, McCollum MA, Reno PL, Rosenman BA. 2003. Developmental biology and human evolution. Annu Rev Anthropol 32:85–109.
Marotti G. 1963. Quantitative studies on bone reconstruction. 1. The reconstruction in homotypic shaft bones. Acta Anat 52: 291–333.
Marotti G. 1976. Map of bone formation rate values recorded throughout the skeleton of the dog. In: Jaworski ZFG, editor. Proc 1st Workshop on Bone Morphometry. Ottawa: Ottawa University Press. p 202–207.
Marotti G. 1996. The structure of bone tissues and the cellular control of their deposition. Ital J Anat Embryol 101:25–79.
Marotti G, Zallone AZ. 1980. Changes in the vascular network during the formation of Haversian systems. Acta Anat 106:84–100.
Martin RB. 1993. Aging and strength of bone as a structural material. Calcif Tissue Int 53(Suppl 1):S34–S40.
Martin RB. 2000. Toward a unifying theory of bone remodeling. Bone 26:1–6.
Martin RB. 2002. Is all cortical bone remodeling initiated by microdamage? Bone 30:8–13.
Martin RB, Burr DB. 1989. Structure, function and adaptation of compact bone. New York: Raven Press. p 1–275.
Martin RB, Mathews PV, Lau ST, Gibson VA, Stover SM. 1996. Collagen fiber organization is related to mechanical properties and remodeling in equine bone. A comparison of two methods. J Biomech 29:1515–1521.
Martin RB, Burr DB, Sharkey NA. 1998. Skeletal tissue mechanics. New York: Springer. p 1–392.
Mason MW, Skedros JG, Bloebaum RD. 1995. Evidence of strain-mode-related cortical adaptation in the diaphysis of the horse radius. Bone 17:229–237.
McMahon JM, Boyde A, Bromage TB. 1995. Pattern of collagen fiber orientation in the ovine calcaneal shaft and its relation to locomotor-induced stain. Anat Rec 242:147–158.
Mullender MG, Huiskes R. 1997. Osteocytes and bone lining cells: which are the best candidates for mechano-sensors in cancellous bone? Bone 20:527–532.
Nagurka ML, Hayes SC. 1980. An interactive graphics package for calculating cross-sectional properties of complex shapes. J Biomech 13:59–64.
Norman TL, Wang Z. 1997. Microdamage of human cortical bone: Incidence and morphology in long bones. Bone 20:375–379.
Norman TL, Vashishth D, Burr DB. 1995. Fracture toughness of human bone under tension. J Biomech 28:309–320.
Norman TL, Nivargikar SV, Burr DB. 1996. Resistance to crack growth in human cortical bone is greater in shear than in tension. J Biomech 29:1023–1031.
O'Connor JA, Lanyon LE, MacFie H. 1982. The influence of strain rate on adaptive bone remodeling. J Biomech 15:767–781.
Papadimitriou HM, Swartz SM, Kunz TH. 1996. Ontogenetic and anatomic variation in mineralization of the wing skeleton of the Mexican free-tailed bat, *Tadarida brasiliensis*. J Zool Lond 240:411–426.
Parfitt AM, Mundy GR, Roodman GD, Hughes DE, Boyce BF. 1996. A new model for the regulation of bone resorption, with particular reference to the effects of bisphosphonates. J Bone Miner Res 11:150–159.
Pattin CA, Caler WE, Carter DR. 1996. Cyclic mechanical property degradation during fatigue loading of cortical bone. J Biomech 29:69–79.
Petrtýl M, Heřt J, Fiala P. 1996. Spatial organization of the Haversian bone in man. J Biomech 29:161–169.

Pfeiffer S. 1998. Variability in osteon size in recent human populations. Am J Phys Anthropol 106:219–227.
Purdue JR. 1983. Epiphyseal closure in white-tailed deer. J Wildlife Manag 47:1207–1213.
Raff MC. 1996 Size control: the regulation of cell numbers in animal development. Cell 86:173–175.
Rayner JMV. 1985. Linear relations in biomechanics: the statistics of scaling functions. J Zool (Lond) A 206:415–439.
Reilly DT, Burstein AH. 1974. The mechanical properties of cortical bone. J Bone Joint Surg 56-A:1001–1022.
Reilly GC. 2000. Observations of microdamage around osteocyte lacunae in bone. J Biomech 33:1131–1134.
Reilly DT, Burstein AH. 1975. The elastic and ultimate properties of compact bone tissue. J Biomech 8:393–405.
Reilly GC, Currey JD. 1999. The development of microcracking and failure in bone depends on the loading mode to which it is adapted. J Exp Biol 202:543–552.
Reilly GC, Currey JD. 2000. The effects of damage and microcracking on the impact strength of bone. J Biomech 33:337–343.
Reilly GC, Currey JD, Goodship AE. 1997. Exercise of young thoroughbred horses increases impact strength of the third metacarpal bone. J Orthop Res 15:862–868.
Richman EA, Ortner DJ, Schulter-Ellis FP. 1979. Differences in intracortical bone remodeling in three aboriginal American populations: possible dietary factors. Calcif Tissue Int 28:209–214.
Riggs CM, Lanyon LE, Boyde A. 1993a. Functional associations between collagen fibre orientation and locomotor strain direction in cortical bone of the equine radius. Anat Embryol 187: 231–238.
Riggs CM, Vaughan LC, Evans GP, Lanyon LE, Boyde A. 1993b. Mechanical implications of collagen fibre orientation in cortical bone of the equine radius. Anat Embryol 187:239–248.
Robling AG, Stout SD. 1999. Morphology of the drifting osteon. Cells Tissues Organs 164:192–204.
Rodríguez JI, Carcia-Alix A, Palacios J, Paniagua R. 1988a. Changes in the long bones due to fetal immobility caused by neuromuscular disease. J Bone Joint Surg 76-A:1052–1060.
Rodríguez JI, Palacios J, Carcia-Alix A, Pastor I, Paniagua R. 1988b. Effects of immobilization of fetal bone development. A morphometric study in newborns with congenital neuromuscular diseases with intrauterine onset. Calcif Tissue Int 43:335–339.
Rodríguez JI, Palacios J, Ruiz A, Sanchez M, Alvarez I, Demiguel E. 1992. Morphological changes in long bone development in fetal akinesia deformation sequence: an experimental study in curarized rat fetuses. Teratology 45:213–221.
Rubin CT. 1984. Skeletal strain and the functional significance of bone architecture. Calcif Tissue Int 36:11–18.
Rubin CT, Lanyon LE. 1984. Dynamic strain similarity in vertebrates: An alternative to allometric limb bone scaling. J Theor Biol 107:321–327.
Rubin CT, Lanyon LE. 1985. Regulation of bone mass by mechanical strain magnitude. Calcif Tissue Int 37:411–417.
Rubin CT, McLeod KJ, Bain SD. 1990. Functional strains and cortical bone adaptation: Epigenetic assurance of skeletal integrity. J Biomech 23:43–54.
Rubin CT, McLeod KJ, Gross TS, Donahue HJ. 1992. Physical stimuli as potent determinants of bone morphology. In: Carlson DS, Goldstein SA, editors. Bone biodynamics in orthodontic and orthopedic research. Ann Arbor: University of Michigan. p 75–91.
Rubin CT, Fritton S, Sun YQ, McLeod K. 1996. Biomechanical parameters which stimulate bone formation: the ugly duckling of the skeletal growth factors. In: Davidovitch Z, Norton LA, editors. Biological mechanisms of tooth movement and craniofacial adaptation. Boston: Harvard Society for the Advancement of Orthodontics. p 51–59.
Ruff CB. 1981. Structural changes in the lower limb bones with aging at Pecos Pueblo. Ph.D. Dissertation. Philadelphia: University of Pennsylvania.
Ruff CB. 1983. The contribution of cancellous bone to long bone strength and rigidity. Am J Phys Anthropol 61:141–143.
Ruff CB. 1989. New approaches to structural evolution of limb bones in primates. Folia Primatol 53:142–159.
Ruff CB, Hayes WC. 1983. Cross-sectional geometry of Pecos Pueblo femora and tibiae — a biomechanical investigation. 1. Method and general patterns of variation. Am J Phys Anthropol 60:359–381.
Schaffler MD, Burr DB. 1988. Stiffness of compact bone: effects of porosity and density. J Biomech 21:13–16.
Schaffler MB, Burr DB, Jungers WL, Ruff CB. 1985. Structural and mechanical indicators of limb specialization in primates. Folia Primatol (Basel) 45:61–75.
Schaffler MB, Radin EL, Burr DB. 1989. Mechanical and morphological effects of strain rate on fatigue of compact bone. Bone 10:207–214.
Schaffler MB, Radin EL, Burr DB. 1990. Long-term fatigue behavior of compact bone at low strain magnitude and rate. Bone 11:321–326.
Schmid E. 1972. Atlas of animal bones: for prehistorians, archaeologists and quaternary geologists. New York: Elsevier.
Shelton DR, Gibeling JC, Martin RB, Stover SM. 2000. Fatigue crack growth rates in equine cortical bone. Conference Proceedings of the American Society of Biomechanics (24th Annual Meeting), Chicago. p 247–248.
Skedros JG. 1994. Collagen fiber orientation in skeletal tension/compression systems: a potential role of variant strain stimuli in the maintenance of cortical bone organization. J Bone Miner Res 9:S251.
Skedros JG. 2000. Do BMUs adapt osteon cross-sectional shape for habitual tension vs. compression loading? J Bone Miner Res 15(Suppl 1):S347.
Skedros JG. 2001. Collagen fiber orientation: a characteristic of strain-mode-related regional adaptation in cortical bone. Bone 28:S110–S111
Skedros JG, Brady J. 2001. Ontogeny of cancellous bone anisotropy in a natural "trajectorial" structure: genetics or epigenetics? J Bone Miner Res 16(Suppl 1):73.
Skedros JG, Kuo TY. 1999. Ontogenetic changes in regional collagen fiber orientation suggest a role for variant strain stimuli in cortical bone construction. J Bone Miner Res 14(Suppl 1): S441.
Skedros JG, Ota D, Bloebaum RD. 1993a. Mineral content analysis of tension/compression skeletal systems: indications of potential strain-specific differences. J Bone Miner Res 8:789.
Skedros JG, Bloebaum RD, Bachus KN, Boyce TM, Constantz B. 1993b. Influence of mineral content and composition on gray-levels in backscattered electron images of bone. J Biomed Mater Res 27:57–64.
Skedros JG, Bloebaum RD, Mason MW, Bramble DM. 1994a. Analysis of a tension/compression skeletal system: possible strain-specific differences in the hierarchical organization of bone. Anat Rec 239:396–404.
Skedros JG, Mason MW, Bloebaum RD. 1994b. Differences in osteonal micromorphologies between tensile and compressive cortices of a bending skeletal system: indications of potential strain-specific differences in bone microstructure. Anat Rec 239:405–413.
Skedros JG, Chow F, Patzakis MJ. 1995. The artiodactyl calcaneus as a model for examining mechanisms governing regional differences in remodeling activities in cortical bone. J Bone Miner Res 10(Suppl):S441.
Skedros, JG, Mason MW, Nelson MC, Bloebaum RD. 1996a. Evidence of structural and material adaptation to specific strain features in cortical bone. Anat Rec 246:47–63.
Skedros JG, Dietch KC, Zirovich MD, Mason MW. 1996b. Uniform osteocyte lacuna population densities in a limb bone with non-uniform customary strain milieu and heterogeneous material organization. J Bone Miner Res 11(Suppl 1):S268.
Skedros JG, Su SC, Bloebaum RD. 1997. Biomechanical implications of mineral content and microstructural variations in cortical bone of horse, elk and sheep calcanei. Anat Rec 249:297–316.

Skedros JG, Hughes PE, Zirovich MD. 1998. Collagen fiber orientation in the turkey ulna supports a role for variant strain stimuli in cortical bone construction. Bone 23(Suppl 5):S437.

Skedros JG, Hughes PE, Nelson K, Winet H. 1999. Collagen fiber orientation in the proximal femur: challenging Wolff's tension/compression interpretation. J Bone Miner Res 14(Suppl 1): S441.

Skedros JG, Dayton MR, Bachus KN. 2000a. Relative effects of collagen fiber orientation, mineralization, porosity, and percent and population density of osteonal bone on equine cortical bone mechanical properties in mode-specific loading. Proc American Society of Biomechanics; 24th Annual Meeting, Chicago. p 173–174.

Skedros JG, Hunt KJ, Attaya EN, Zirovich MD. 2000b. Uniform osteocyte lacuna population densities in a limb bone with highly non-uniform strain milieu. J Bone Miner Res 15(Suppl 1):S347.

Skedros JG, Takano Y, Turner CH. 2000c. Mechanical loading patterns determine collagen and mineral orientation. J Bone Miner Res 15(Suppl 1):S348.

Skedros JG, Mason MW, Bloebaum RD. 2001a. Modeling and remodeling in a developing artiodactyl calcaneus: a model for evaluating Frost's Mechanostat hypothesis and its corollaries. Anat Rec 263:167–185.

Skedros JG, Hunt KJ, Bloebaum RD. 2001b. Expanding Wolff's law: variant and invariant strain stimuli in bone adaptation and maintenance. Trans Orthop Res Soc 26:548.

Skedros JG, Dayton MR, Bachus KN. 2001c. Strain-mode-specific loading of cortical bone reveals an important role for collagen fiber orientation in energy absorption. Trans Orthop Res Soc 26:519.

Skedros JG, Hunt KJ, Dayton MT, Bloebaum RD, Bachus KN. 2001d. Relative contributions of material characteristics to failure properties of cortical bone in strain-mode-specific loading: implications for fragility in osteoporosis and aging. Trans Am Soc Biomech 25:215–216.

Skedros JG, Hunt KJ, Sybrowsky CL. 2002a. Ontogenetic development of the ovine calcaneus: a model for examining the relative contributions of genetic, epigenetic, and extra-genetic stimuli. J Bone Miner Res 17:S330.

Skedros JG, Brady J, Sybrowsky C. 2002b. Mathematical analysis of trabecular trajectories in apparent trajectorial structures: the unfortunate historical emphasis on the human proximal femur. Am J Phys Anthropol 33(Suppl):142.

Skedros JG, Hunt KJ, Dayton MR, Bloebaum RD, Bachus KN. 2003a. The influence of collagen fiber orientation on mechanical properties of cortical bone of an artiodactyl calcaneus: implications for broad applications in bone adaptation. Trans Orthop Res Soc 28:411.

Skedros JG, Sybrowsky CL, Dayton MR, Bloebaum RD, Bachus KN. 2003b. The role of osteocyte lacuna population density on the mechanical properties of cortical bone. Trans Orthop Res Soc 28:414.

Skedros JG, Sybrowsky CL, Parry TR, Bloebaum RD. 2003c. Regional differences in cortical bone organization and microdamage prevalence in Rocky Mountain mule deer. Anat Rec 274A:837–850.

Skedros JG, Dayton MR, Sybrowsky CL, Bloebaum RD, Bachus KN. 2003d. Are uniform regional safety factors an objective of adaptive modeling/remodeling in cortical bone? J Exp Biol 206: 2431–2439.

Skerry T. 2000. Biomechanical influences on skeletal growth and development. In: O'Higgins P, Cohn MJ, editors. Development, growth, and evolution: implications for the study of the hominid skeleton. San Diego: Academic Press. p 29–40.

Skerry TM, Suswillo R, El Hay AJ, Ali NN, Dodds RA, Lanyon LE. 1990. Load-induced proteoglycan orientation in bone tissue in vivo and in vitro. Calcif Tissue Int 46:318–326.

Smit TH, Burger EH. 2000. Is BMU-coupling a strain-regulated phenomenon? A finite element analysis. J Bone Miner Res 15:301–307.

Smit TH, Burger EH, Huyghe JM. 2002. A case for strain-induced fluid flow as a regulator of BMU-coupling and osteonal alignment. J Bone Miner Res 17:2021–2029.

Srinivasan S, Gross TS. 2000. Canalicular fluid flow induced by bending of a long bone. Med Eng Phys 22:127–133.

Stout SD. 1984. Intraskeletal variation in osteon remodeling. Am J Phys Anthropol 63:223.

Stover SM, Pool RR, Martin RB, Morgan JP. 1992. Histological features of the dorsal cortex of the third metacarpal bone mid-diaphysis during postnatal growth in thoroughbred horses. J Anat 181:455–469.

Su S. 1998. Microstructure and mineral content correlations to strain parameters in cortical bone of the artiodactyl calcaneus. Masters thesis, Salt Lake City: University of Utah.

Su M, Borke JL, Donahue HJ, Li Z, Warshawsky NM, Russell CM, Lewis JE. 1997. Expression of connexin 43 in rat mandibular bone and peridontal ligament (PDL) cells during experimental tooth movement. J Dent Res 76:1357–1366.

Su S, Skedros JG, Bloebaum RD, Bachus KN. 1999. Loading conditions and cortical construction of an artiodactyl calcaneus. J Exp Biol 202:3239–3254.

Sumner DR. 1984 Postembryonic dimensional allometry of the human femur. Am J Phys Anthropol 64:69–74.

Swartz SM. 1990. Curvature of the forelimb bones of anthropoid primates: overall allometric patterns and specializations in suspensory species. Am J Phys Anthropol 83:477–498.

Swartz SM, Biewener AA. 1992. Shape and scaling. In: Biewener AA, editor. Biomechanics — structures and systems: a practical approach. New York: Oxford University Press. p 21–43.

Swartz SM, Bennett MB, Carrier DR. 1992. Wing bone stresses in free flying bats and the evolution of skeletal design for flight. Nature 359:726–729.

Takano Y, Turner CH, Owan I, Martin RB, Lau ST, Forwood MR, Burr DB. 1999. Elastic anisotropy and collagen orientation of osteonal bone are dependent upon the mechanical strain distribution. J Orthop Res 17:59–66.

Taylor D, Lee TC. 1998. Measuring the shape and size of microcracks in bone. J Biomech 31:1177–1180.

Terai K, Takano-Yamamoto T, Ohba Y, Hiura K, Sugimoto M, Sato M, Kawahata H, Inaguma N, Kitamura Y, Nomura S. 1999. Role of osteopontin in bone remodeling caused by mechanical stress. J Bone Miner Res 14:839–849.

Torzilli PC, Takebe K, Burstein AH, Heiple KG. 1981. Structural properties of immature canine bone. J Biomech Eng 103:232–238.

Turner CH. 1991. Homeostatic control of bone structure: an application of feedback theory. Bone 12:203–217.

Turner CH. 1999. Toward a mathematical description of bone biology: the principle of cellular accommodation. Calcif Tissue Int 65:466–471.

Turner CH, Wang T, Burr DB. 2001. Shear strength and fatigue properties of human cortical bone determined from pure shear tests. Calcif Tissue Int 69:373–378.

van der Meulen, MCH, Ashford MW Jr, Kiratli BJ, Bachrach LK, Carter DR. 1996. Determinants of femoral geometry and structure during adolescent growth. J Orthop Res 14:22–29.

Vashishth D, Verborgt O, Divine G, Schaffler MB, Fyhrie DP. 2000. Decline in osteocyte lacunar density in human cortical bone is associated with accumulation of microcracks with age. Bone 26:375–380.

Wainwright SA, Biggs WD, Currey JD, Gosline JM. 1982. Elements of structural systems. In: Mechanical design in organisms. Princeton, NJ: Princeton University Press. p 254–258.

Wolpert L. 1981. Positional information and pattern formation. Philos Trans R Soc Lond B Biol Sci 295:441–450.

Wolpert L. 1996. One hundred years of positional information. Trends Genet 12:359–364.

Wolpert L, Beddington R, Brockes J, Jessell T, Lawrence P, Meyerowitz E. 1998. Principles of development. Oxford: Oxford Press.

Woo SLY, Keui SC, Amiel D, Gomez MA, Hayes WC, White FC, Akeson WH. 1981. The effect of prolonged physical training on the properties of long bone: a study of Wolff's law. J Bone Joint Surg. 63-A:780–787.

Wright TM, Hayes WC. 1976. Tensile testing of bone over a wide range of strain rates: effects of strain rate, microstructure and density. Med Biol Eng 14:671–680.
Yeh CK, Rodan GA. 1984. Tensile forces enhance prostaglandin E synthesis in osteoblasts grown on collagen ribbons. Calcif Tissue Int 36(Suppl):67–71.
Yeni YN, Norman TL. 2000. Fracture toughness of human femoral neck: Effect of microstructure, composition, and age. Bone 26:499–504.
Yeni, YN, Brown CU, Wang Z, Norman TL. 1997. The influence of bone morphology on fracture toughness of the human femur and tibia. Bone 21:453–459.
Yeni YN, Vashishth D, Fyhrie DP. 2001. Estimation of bone matrix apparent stiffness variation caused by osteocyte lacunar size and density. J Biomech Eng 123:10–17.
Zioupos P, Currey JD. 1998. Changes in the stiffness, strength, and toughness of human cortical bone with age. Bone 22:57–66.

APPENDIX
Definitions

Adaptation: Adaptation in cortical bone commonly refers to either: 1) changes in bone structure and/or material organization in response to loading conditions outside a normal physiologic stress/strain range, distribution, and/or duration (e.g., Lanyon et al., 1979; Woo et al., 1981; Currey, 1984a; Schaffler et al., 1985; Martin and Burr, 1989; Biewener and Bertram, 1994); or 2) the presence of regional differences in structural and/or material organization that are strongly influenced by normal functional stimuli occurring during *normal* development within or between bones (e.g., Currey, 1984a; Martin and Burr, 1989; Bertram and Swartz, 1991; Riggs et al., 1993a,b; Skedros et al., 1994a,b). In the present investigation, "adaptations" are considered to be biomechanically relevant regional variations and temporal changes in cortical bone structural and material organization that are produced by modeling and remodeling processes during *normal* skeletal development. In addition to being mediated by genetic and epigenetic influences, which are heritable, these processes may be influenced by nonheritable ("extragenetic") stimuli such as regional variations in microdamage incidence.

Bone microstructure: Examples of microstructural characteristics include: 1) secondary osteon population density; 2) osteon cross-sectional diameter and shape; 3) fractional area of secondary bone; 4) porosity (e.g., osteocyte lacunae, central canals of secondary osteons, Volkmann's canals, and other vascular spaces); and 5) osteocyte lacunar-canalicular geometries. Most microstructural characteristics are produced by bone *remodeling* processes.

Bone structural organization: This refers to bone geometry and includes curvature, cross-sectional area, cross-sectional shape and related dimensions (including moments of inertia), and cortical thickness. Most structural characteristics are produced by bone *modeling* processes.

Bone ultrastructure: Examples include: 1) predominant collagen orientation, organization, and inter- and intramolecular cross-linking; and 2) topographic distribution of noncollagenous proteins.

Fatigue: The number of cycles required for failure of a bone or bone specimen at a particular load level. The basic means of presenting fatigue data is an "S-N plot" of the applied stress or strain vs. the number of cycles required for failure at that load level (see Martin et al., 1998). Fatigue damage can be manifested as microcracks and ultrastructural and molecular damage.

Fatigue Resistance: The ability of bone to resist fatigue failure and resist or accommodate the formation of fatigue damage (e.g., microcracks, ultrastructural failure, molecular damage).

Modeling: Adaptations resulting from *modeling* activities include the accretion and/or resorption of secondary or nonsecondary bone (e.g., circumferential lamellae and trabecular bone in some cases) on periosteal or endosteal surfaces. They are detected as changes and/or differences in a bone's curvature, cross-sectional shape, and/or regional cortical thickness.

Remodeling: Adaptations produced by remodeling activities involve the replacement of intracortical bone; this is achieved through the activation of basic multicellular units (BMUs) that create secondary osteons (Haversian systems) in cortical bone (Frost, 1986; Jee et al., 1991; Parfitt et al., 1996). Manifestations of remodeling adaptations may include regional changes and/or differences in secondary osteon population density (N.On/Ar), fractional area of secondary bone (On.B/Ar), cross-sectional area of individual secondary osteons (On.Ar), and/or porosity. If a bone has increased On.B/Ar, then the bone is more "remodeled." In contrast, "remodeling" connotes an active renewal process (Parfitt et al., 1996). Remodeling rates are thought to be the primary determinant of mineralization differences in the bone matrix within the cortices of many bones (Grynpas, 1993; Martin, 1993). A relatively increased remodeling rate in a region of bone is detected in the present investigation as relatively decreased bone matrix mineral content and increased population densities of resorption spaces and newly forming secondary osteons (Skedros et al., 1997).

Toughness: A material property that reflects the ability to resist crack growth and withstand brittle fracture from an applied single load. Toughness is a function of applied stress, size of material flaws, and geometrical thickness (Martin and Burr, 1989). This contrasts with energy density absorption, a measurement of work-to-failure. An example in terms of mineral content would be a highly mineralized material that absorbs a large amount of energy to failure, typically exhibiting brittle failure (very little energy absorbed postyield) vs. a less mineralized, less stiff material which, although may or may not absorb a high amount of energy to failure, undergoes a greater degree of postyield strain, thereby exhibiting fracture toughness (Currey, 1984a).